

This is the peer reviewed version of the following article: [Penna, D., Zuecco, G., Crema, S., Trevisani, S., Cavalli, M., Pianezzola, L., Marchi, L. & Borga, M. 2017, "Response time and water origin in a steep nested catchment in the Italian Dolomites", *Hydrological Processes*, vol. 31, no. 4, pp. 768-782.], which has been published in final form at [<https://doi.org/10.1002/hyp.11050>]. This article may be used for non-commercial purposes in accordance with Wiley Terms and Conditions for Use of Self-Archived Versions. This article may not be enhanced, enriched or otherwise transformed into a derivative work, without express permission from Wiley or by statutory rights under applicable legislation. Copyright notices must not be removed, obscured or modified. The article must be linked to Wiley's version of record on Wiley Online Library and any embedding, framing or otherwise making available the article or pages thereof by third parties from platforms, services and websites other than Wiley Online Library must be prohibited."

Response time and water origin in a steep nested catchment in the Italian Dolomites

Journal:	<i>Hydrological Processes</i>
Manuscript ID	HYP-16-0376.R1
Wiley - Manuscript type:	Research Article
Date Submitted by the Author:	03-Oct-2016
Complete List of Authors:	Penna, Daniele; University of Florence, Department of Agricultural, Food and Forestry Systems Zuecco, Giulia; University of Padova, Department of Land, Environment, Agriculture and Forestry Crema, Stefano; National Research Council, IRPI Trevisani, Sebastiano; University IUAV of Venice, DACC Cavalli, Marco; CNR, IRPI; Pianezzola, Luisa; University of Padova, Land, Environment, Agriculture and Forestry Marchi, Lorenzo; CNR, IRPI; Borga, Marco; University of Padova, Department of Land and Agroforest Environments;
Keywords:	water origin, isotopes, electrical conductivity, flow pathways, nested catchment, time of rise

SCHOLARONE™
Manuscripts

Response time and water origin in a steep nested catchment in the Italian Dolomites

Short title: Response time and water origin in a nested catchment

Daniele Penna¹, Giulia Zuecco², Stefano Crema³, Sebastiano Trevisani⁴, Marco Cavalli³, Luisa Pianezzola², Lorenzo Marchi³, Marco Borga²

¹ Department of Agricultural, Food and Forestry Systems, University of Florence, via San Bonaventura 13, 50145, Florence-Firenze, Italy.

² Department of Land, Environment, Agriculture and Forestry, University of Padova, viale dell'Università 16, 35020 Legnaro (PD), Italy

³ National Research Council (CNR) - Research Institute for Geo-Hydrological Protection (IRPI), Corso Stati Uniti 4, 35127, Padova, Italy

⁴ DACC Department, University IUAV of Venice, Dorsoduro 2206, 30123 Venezia, Italy

Corresponding author: Daniele Penna (daniele.penna@unifi.it)

Abstract

In this study we investigate the surface flow time of rise in response to rainfall and snowmelt events at different spatial scales and the main sources originating channel runoff and spring water in a steep nested headwater catchment (Rio Vauz, Italian Dolomites), characterized by a marked elevation gradient. We monitored precipitation at different elevations and measured water stage/streamflow at the outlet of two rocky subcatchments of the same size, representative of the upper part of the catchment dominated by outcropping bedrock, at the outlet of a soil-mantled and vegetated subcatchment of similar size but different morphology, and by the outlet of the main catchment. Hydrometric data are coupled with stable isotopes and electrical conductivity sampled from different water sources during five years, and used as tracers in end-member mixing analysis,

application of the two component mixing model and analysis of the slope of the dual-isotope regression line. Results reveal that times of rise are slightly shorter for the two rocky subcatchments, particularly for snowmelt and mixed rainfall/snowmelt events, compared to the soil-mantled catchment and the entire Rio Vauz catchment. The highly-variable tracer signature of the different water sources reflects the geomorphological and geological complexity of the study area. The principal end-members for channel runoff and spring water are identified in rainfall and snowmelt, which are the dominant water sources in the rocky upper part of the study catchment, and soil water and shallow groundwater, which play a relevant role in originating baseflow and spring water in the soil-mantled and vegetated lower part of the catchment. Particularly, snowmelt contributes up to $64\% \pm 8\%$ to spring water in the concave upper parts of the catchment and up to $62\% \pm 11\%$ to channel runoff in the lower part of the catchment. These results offer new experimental evidences on how Dolomitic catchments capture and store rain water and meltwater, releasing it through a complex network of surface and subsurface flow pathways, and allow for the construction of a preliminary conceptual model on water transmission in snowmelt-dominated catchments featuring marked elevation gradients.

Keywords: time of rise; water origin; isotopes; electrical conductivity; flow pathways; nested catchment.

1 Introduction

Headwater catchments in mountain regions play a number of valuable environmental roles. Given their typical small size ($< 10 \text{ km}^2$) and morphological and pedological characteristics (steep hillslopes, narrow valley bottoms and shallow soils) they comprise source areas of water, sediments and solutes and, at the same time, act as transitory hydrological sinks (Sidle et al., 2000; Payn et al., 2012). Headwater streams are responsible of transport mechanisms for different materials including

1
2 53 nutrients, organic matter, wood and aquatic species (Wipfli et al., 2007; Sando and Blasch, 2015)
3
4 54 affecting downstream water quality and ecosystem health (Bishop et al., 2008; Mueller et al., in
5
6 55 press). Mountain headwater catchments, especially those that are dominated by snowmelt and ice
7
8 56 melt dynamics, are generally water-rich but, often due to logistical inconveniences, are data-poor
9
10 57 (Beniston et al., 1997). Thus, our understanding of how mountain headwater catchments capture
11
12 58 and store rain water and meltwater and then release it through surface and subsurface flow
13
14 59 pathways is still meagre. Increasing our knowledge about fundamental processes such as the timing
15
16 60 of the stream response to rainfall and snowmelt events and the origin of water sources that generate
17
18 61 surface and subsurface runoff is therefore a critical step in order to improve water resources
19
20 62 management strategies in mountain regions, especially under the current global warming conditions
21
22 63 to which these environments are particularly sensitive (Knowles et al., 2015).
23
24
25
26 64
27
28 65 Catchment response time integrates the effects of all factors that control the travel time of water
29
30 66 input to the outlet, such as catchment size, morphology, slope, land cover, soil properties and
31
32 67 geology (Dingman, 2002). Therefore, catchment response time, expressed by the lag time between
33
34 68 rainfall or snowmelt (input) and streamflow (output), is an important indicator of the catchment
35
36 69 hydrological properties and provides useful insights to understand runoff generation processes
37
38 70 (Haga et al., 2005). The analysis of response time conducted in headwater catchments has revealed
39
40 71 that different controls act on lag times. For humid catchments where the hydrological response was
41
42 72 dominated by subsurface flow, Montgomery and Dietrich (2002) found that lag times increased
43
44 73 with catchment size and decreased with catchment slope. In granitic headwater catchments in Japan
45
46 74 draining areas up to 6.3 ha, Onda et al. (2001) found that peak streamflow occurred almost at the
47
48 75 same time than peak rainfall, but that in shale and serpentinite catchments with areas up to 5.3 and
49
50 76 7.3 ha lag times to peak streamflow were much longer. For other Japanese steep headwater
51
52 77 catchments underlain by granitic rock, Haga et al. (2005) identified two types of response time
53
54 78 related to different antecedent soil moisture conditions and rainfall amount and intensity: for events
55
56
57
58
59
60

with short lag time (<2 hours) saturation excess overland flow was dominant whereas for events with longer lag time (>24 hours) saturated subsurface flow above the soil-bedrock interface was the principal runoff generation process. However, Meyles et al. (2003) observed that lag times in a small headwater catchment in UK were poorly related to antecedent conditions and were predominantly a function of the characteristics of rainstorms. In the humid Maimai headwater catchment in New Zealand, McGlynn et al. (2004) found that during a small rainfall event, runoff was generated primarily in headwater riparian zones, streamflow peaks became damped and lag times increased in a downstream direction consistently with catchment size. On the contrary, for a large event, runoff was generated more uniformly and lag times were more consistent across scale (McGlynn et al., 2004). Finally, in forested headwater catchments it was observed that pipe flow can increase discharge from hillslopes and therefore decrease the lag times of the storm hydrograph (Uchida et al., 2001).

The analysis of water origin and dominant hydrological pathways in headwater catchments can greatly benefit from the use of environmental tracers, such as stable isotopes of water (^2H and ^{18}O) and electrical conductivity (EC). Recent studies have adopted tracer-based techniques such as end-member mixing analysis (EMMA) and mixing models to investigate water origin, mixing processes, flow pathways and runoff components in meltwater-dominated (snowmelt and/or glacier melt) mountain catchments. For instance, some researchers have employed isotopic and hydrochemical tracers to assess the sources of streamflow and quantify snowmelt and glacier melt contributions to runoff at the monthly or seasonal scale (Jeelani et al., 2013; Liu et al., 2013; Ohlanders et al., 2013; Liu and Liao, in press), even for different years (Maurya et al., 2011; Liu et al., 2012; Dahlke et al., 2014), during spring snowmelt (Jin et al., 2012), or melt-induced runoff events (Engel et al., 2016; Penna et al., 2016). Other studies have used tracers to identify the role of meltwater in spring recharge (Jeelani et al., 2010; Penna et al., 2014b; Šanda et al., 2014; Liu et al., 2015; Meng et al., 2015) and to assess the impact of snowmelt in different parts of the catchment

1
2 105 (Holko et al., 2013). Other opportunities to determine stream water source components and obtain
3
4 106 insights into the catchment hydrological functioning derive from adopting the dual-isotope
5
6 107 approach (Klaus et al., 2015), based on the analysis of the slope of $\delta^2\text{H}$ - $\delta^{18}\text{O}$ regression lines, which
7
8 108 has been limitedly used in steep snowmelt-dominated headwater catchments.
9
10
11 109 Indeed, despite the amount of previous work in headwater catchments, very little is known about
12
13 110 catchment response time, origin of water and the main hydrological flow pathways in high-
14
15 111 elevation nested catchments characterized by a strong elevation gradient and different land cover.
16
17 112 This is true especially in Dolomitic regions where karst processes noticeably affect storage and
18
19 113 create preferential flow routes. In this paper, we use hydrometric and tracer data collected in the Rio
20
21 114 Vauz Catchment, in the Italian Dolomites, to address the following questions:
22
23
24 115 i) are response times of nested catchments different according to the catchment size, slope and land
25
26 116 cover?
27
28 117 ii) what are the main water sources that contribute to channel runoff and spring water at different
29
30 118 spatial scales?
31
32 119 iii) what is the role of snowmelt on spring recharge and channel runoff in the upper part of the
33
34 120 catchment?
35
36
37 121

38
39 122 **2 Study area**

40
41 123 **2.1 Rio Vauz Catchment**

42
43 124 The Rio Vauz Catchment (RVC, 1.9 km²) is located in the Dolomites, Eastern Italian Alps (Fig. 1).
44
45 125 The site ranges in elevations between 1847 m a.s.l. at the outlet and 3152 m a.s.l. on the top of the
46
47 126 main peak (Piz Boè). Average monthly temperatures vary between -5.7 °C in January and 14.1 °C
48
49 127 in July. Mean annual precipitation is about 1220 mm, 49% is in form of snow. April, May and
50
51 128 sometimes June are characterized by high flow conditions due to snowmelt but summer
52
53 129 thunderstorms and autumn precipitation determine important flood events as well. The upper part of
54
55 130 the catchment (from to the top to roughly 2200 m a.s.l.) is dominated by subvertical Dolomitic rock
56
57
58
59
60

1 cliff whereas the central and lower part are vegetated by alpine grassland and sparse European
2
3
4 132 larches and Norway spruces. The area is characterised by a prevalence of Triassic calcareous rocks
5
6 133 with characteristic peaks of stratified and structurally deformed dolomite rocks (Bosellini et al.,
7
8 134 2003; Doglioni and Carminati, 2008). The morphology of the study site is deeply influenced by the
9
10 135 geo-structural setting, both in relation to the different lithological geo-mechanical characteristics as
11
12 136 well as in relation to the characteristics of structural discontinuities (fractures, faults, strata,
13
14 137 lamination). The most resistant rocks, which outcrop in the upper part of the catchment, belong to
15
16 138 the dolomite and limestone formations (the main ones are “Dolomia Principale” and “Dolomia
17
18 139 Cassiana”). The rocks of the other formations, i.e., “Travenanzes” and “San Cassiano”, are weaker,
19
20 140 and this reflects in gentler slopes, strong deformation, widespread presence of landslides and
21
22 141 erosional processes (Fig. S1). The patterns of the stream network are deeply influenced by structural
23
24 142 lineaments, with main channels developed along major fault lines (Marchi et al., 2008; 2015). The
25
26 143 main aquifers are represented by carbonate aquifers corresponding to the “Dolomia Principale” and
27
28 144 “Dolomia Cassiana” formations; minor aquifers are formed by the quaternary deposits constituted
29
30 145 by scree slopes and alluvial and colluvial deposits. The hydrogeological conceptual framework of
31
32 146 the area can be exemplified as composed by two main superposed carbonate aquifers, with the
33
34 147 upper aquifer corresponding to “Dolomia Principale” and the lower one to “Dolomia Cassiana”,
35
36 148 respectively delimited at the bed by the lower permeability formations of “Travenanzes” and “San
37
38 149 Cassiano”. Both aquifers are characterized by the presence of free draining and dammed springs
39
40 150 (Williams and Ford, 2007), emerging at various elevations. The strata are mainly sub-horizontal,
41
42 151 slightly dipping South-East, toward the outlet of RVC. The two main dolomite aquifers can be
43
44 152 viewed as a triple-porosity system, in which the water storage and transmission are related to the
45
46 153 rock matrix porosity, structural discontinuities (fractures, strata, etc.) and karstic conduits.
47
48 154 Moreover, a possible discontinuous presence of ice bodies in the rock mass above 2600 m a.s.l.
49
50 155 (Mair et al., 2011; Böckli et al., 2012; Krainer et al., 2012; Carturan et al., 2016) may increase the
51
52 156 hydrogeological complexity of the catchment and influence the storage and movement of water.
53
54
55
56
57
58
59
60

2.2 Selected catchments

Within RVC, three subcatchments were selected for the experimental activities (Fig. 1): two rocky subcatchments representative of the upper part, Channel A (ChA) and Channel B (ChB), and one soil-mantled subcatchment in the mid-central part, Bridge Creek Catchment (BCC). ChA and ChB are located in the lower part of the first aquifer at higher elevation, corresponding to the “Dolomia Principale” formation; differently, BCC is located in the lower part of the second aquifer corresponding to the “Dolomia Cassiana” formation. The three subcatchments have similar size but different elevation, lithology, slope and land cover (Table I). Particularly, aerial imagery analysis based on the detection of vegetation cover as a proxy for soil presence indicates an extremely different distribution of soil between the two rocky subcatchments and BCC (Table I). Hypsometric curves highlight a morphological similarity between ChA and ChB, with more than 90% of the area of both catchments falling above 40% of the relative elevation whereas RVC and especially BCC show a more regular distribution and lower hypsometric integrals (Fig. S2). Previous experimental investigations have been conducted at BCC to understand the main runoff generation processes occurring during rainfall and snowmelt events (Penna et al., 2011; 2015; 2016). More information on RVC can be found in other studies (Penna et al., 2013; Camporese et al., 2014).

3 Materials and Methods

3.1 Hydro-meteorological data

The experimental data were collected during five years (2011-2015). Precipitation was measured by not-heated tipping buckets at four locations within RVC: at 2868 m, 2566 m, 2553 m and 1940 m a.s.l.. Rain gauges were typically operated between May and October of each year, except for the highest one which, due to the difficult accessibility of the upper part of the catchment for most of the year, was operated only from June or July to September of each year. In addition, precipitation and air temperature were measured all year round by two heated tipping buckets and temperature

sensors located at 1645 m (Arabba village) and 2155 m a.s.l. (Pordoi Pass), approximately 2.5 km on the East and on the West of RVC, respectively, and operated by the Agency for Environmental Protection of the Veneto Region. For the visual analysis of hydrometric response and tracer response in the study catchment over the entire monitoring period (Section 4.1) the inverse distance weighting (IDW) interpolation method based on precipitation data from the Arabba and Pordoi Pass stations was used. Water stage was measured by pressure transducers installed at the outlet of each subcatchment and at 1888 m a.s.l., close to the outlet of RVC. Streamflow values were available only for BCC where a V-notch weir is installed.

3.2 Sampling for EC and isotopic analysis

Samples for tracer analysis were manually collected from different water sources at various locations (Fig. 1). Samples at ChA, ChB and upper RVC were taken from late June to early October in 2011, 2012, 2013 whereas samples at BCC and lower RVC were collected all year round from 2011 to 2015 (approximately monthly from 2012 to 2015).

Bulk liquid precipitation during the snow-free months was sampled through rainfall collectors located at ChB, upper RVC and by the rain gauge at BCC. Rainfall samplers were equipped with a funnel, a layer of mineral oil to prevent evaporation, and were emptied approximately every month. Shallow groundwater was sampled from two piezometers (named P17 and M26) in the lower part of BCC installed at a depth of 0.60 m and 1.20 m from the soil surface, respectively, in the alluvial and colluvial deposits bordering the creek. Soil water was sampled monthly from May to October from a suction cup installed at 30 cm depth in the riparian zone in the lower part of BCC. Spring water was sampled from one spring in the lower RVC, one spring in the mid-BCC, two springs in the upper RVC, two springs at ChA and five springs at ChB. Channel runoff (stream water) was sampled at five locations at RVC, two locations at BCC and ChA, and one location at ChB. Overall, precipitation was sampled along an elevation gradient from 1940 m to 2868 m a.s.l., spring water from 1917 m to 2947 m a.s.l. and channel runoff from 1845 m to 2848 m a.s.l. Snow was sampled

occasionally in winter at BCC and lower RVC from the snowpack (entire snow core) or from the surface layer after snowfall events. Snow from residual snow patches was also sampled occasionally in summer at ChA and ChB. Snowmelt at BCC was sampled in March and April 2010-2012 from two 1-m² snowmelt samplers (Penna et al., 2016) located at 1943 m and 1957 m a.s.l., and in April and May 2013 by 16 passive capillary samplers (Penna et al., 2014a; Holko et al., 2013) spatially distributed over the riparian zone and lower hillslope zone of BCC. Snowmelt in the upper RVC was sampled from melting snow patches in summer 2011 and 2013. All sampling locations are depicted in Fig. 1.

Samples were collected using 50 ml high-density plastic bottles with a double cap and stored at 4°C. No headspace was left in the bottles whenever possible to minimize evaporation and thus isotopic fractionation. The isotopic composition was determined by laser absorption spectroscopy adopting strategies to increase accuracy and mitigate memory effects (Penna et al., 2010; 2012). The tested instrumental precision is 0.5‰ for $\delta^2\text{H}$ and 0.08‰ for $\delta^{18}\text{O}$. Isotopic values are reported using the δ notation according to the SMOW2-SLAP2 reference scale. EC was measured in the field using a portable conductivity probe with a precision of $\pm 0.1 \mu\text{S}/\text{cm}$ and converted to specific conductance (EC for water temperature to 25°C).

3.3 Event identification and computation of time of rise

The comparative analysis of time of rise, used as a proxy of the response time, in the four catchments was conducted for i) rainfall events, ii) snowmelt events, and iii) mixed events (snowmelt + rainfall) by computing the lag time between the start of the hydrograph rise after the rainfall or snowmelt input and the peak water stage (or the peak streamflow at BCC) (Dingman, 2002). Response time is usually assessed computing the lag time, defined as the time between rainfall centroid or peak rainfall and peak streamflow (Onda et al., 2001; Haga et al., 2005). However, our intention in this study was not only to compare the hydrological dynamics of the four

1
2 235 catchments during rainfall events but also during snowmelt pulses, which typically occur without
3
4 236 rainfall influence. Such a comparison calls for the use of a metric that does not require rainfall data.
5
6 237 Moreover, preliminary analyses showed differences up to 26% among the various rain gauge
7
8 238 measurements, related to the marked elevation range of the catchment. Thus, using the data from
9
10 239 the rain gauge(s) closest to each stream gauge would not make the results easily comparable among
11
12 240 the studied catchments whereas using an interpolated precipitation value would produce noticeable
13
14 241 errors in the lag time computations. In addition, the lack of snowmelt intensity data would prevent
15
16 242 to compute the lag time for snowmelt events. Therefore, in this context, time of rise is used as a tool
17
18 243 to homogeneously characterize and compare the hydrological response of different catchments to
19
20 244 different hydrological inputs.
21
22 245 The procedure to determine the three types of events was based on the detection of a rise in water
23
24 246 stage/streamflow. As a preliminary step, we identified, for each catchment and each monitoring
25
26 247 year, a snowmelt period (typically in spring at BCC, and in late spring-early summer at ChA and
27
28 248 ChB and the outlet of the main catchment) based on the occurrence of regular diurnal cycles in
29
30 249 water stage/streamflow (Lundquist et al., 2005). For each observed flow peak, we assessed i) the
31
32 250 inclusion/exclusion from the snowmelt period; ii) the antecedent temperature, that refers to air
33
34 251 temperature data recorded within 10 hours prior to the flow peak at the weather station closest to
35
36 252 each subcatchment, corrected for the outlet elevation using the lapse rate of 0.6°C/100 m, and that
37
38 253 must be $> 0^{\circ}\text{C}$; iii) the antecedent rainfall, that refers to rainfall data recorded within 5 hours prior
39
40 254 to the flow peak at the weather station closest to each subcatchment (Table II).
41
42 255 The computation of the times of rise was based on the analysis of water stage/streamflow time
43
44 256 series by means of a peak detection function in Matlab® which identifies local maxima and
45
46 257 minima. A threshold to filter out the signal noise, i.e., small fluctuations (around 1-3 mm) due to the
47
48 258 instrumental precision and/or thermal drift occurring during low flow periods, was set. After a first
49
50 259 automatic identification of peaks, a manual check was performed to refine the detection of
51
52 260 minimum values of water stage (or discharge) data that could have been influenced by the noise.
53
54
55
56
57
58
59
60

The time of rise was then computed as the interval between the local minimum before the beginning of the rising limb of the water stage/or streamflow signal, and the subsequent peak. Each flow response for each catchment was assigned to one of the three event types.

3.4 Comparison of the slopes of the $\delta^2\text{H}$ - $\delta^{18}\text{O}$ regression lines

The linear regression between $\delta^2\text{H}$ and $\delta^{18}\text{O}$ data was computed for the different water sources (Table III), following the dual-isotope approach (Klaus and McDonnell, 2015). In order to test whether the slopes of pairs of sample groups (e.g., groundwater in piezometer M26 vs. groundwater in piezometer M27, snowmelt vs. spring water at BCC+lower RVC, snowmelt vs. spring water at ChA+ChB+upper RVC etc.) were statistically different, the test of the comparison of the slopes of $\delta^2\text{H}$ - $\delta^{18}\text{O}$ regression lines from two independent samples with a significance level of 0.01 (Howell, 2010) was applied.

3.5 Two-component mixing model

The estimate of the snowmelt vs. rainfall fraction in channel runoff and spring water was carried out through an isotope-based (^2H) two-component mixing model (Pinder and Jones, 1969; Sklash and Farvolden, 1979). Assuming that channel runoff and spring water are a mixture of rainfall and snowmelt, the equations at the base of the two-component mixing model can be written as follows:

$$1 = sm + rf \tag{Eq. 1}$$

$$\delta_{CR} = sm \cdot \delta_{SM} + rf \cdot \delta_{RF} \tag{Eq. 2}$$

where sm and rf indicate the channel runoff fraction due to snowmelt and rainfall, respectively; the notation δ is the isotopic composition of each component; and the subscripts CR , SM and RF denote channel runoff, snowmelt and rainfall, respectively. Analogously, for spring water (SP), the following equations can be written:

$$\delta_{SP} = sm \cdot \delta_{SM} + rf \cdot \delta_{RF} \tag{Eq. 3}$$

Eqs. 1-3 can be solved for the unknown sm as follows:

$$sm(\%) = \frac{\delta_{CR} - \delta_{RF}}{\delta_{SM} - \delta_{RF}} \cdot 100 \quad (\text{Eq. 4})$$

for channel runoff, and:

$$sm(\%) = \frac{\delta_{SP} - \delta_{RF}}{\delta_{SM} - \delta_{RF}} \cdot 100 \quad (\text{Eq. 5})$$

for spring water. The uncertainty of the estimated snowmelt fractions was computed according to the error propagation method (Genereux, 1998) at the 70% confidence interval. Based on the available dataset, the mixing model in the upper part of RVC was applied to five springs and the outlet of ChA sampled on 5 July 2011, using as δ_{RF} the average isotopic composition of precipitation sampled by the two upper rainfall collectors for the period 5 July-4 August 2011, assuming that the isotopic composition in that period was similar to that in the days antecedent to 5 July. In the lower part of RVC, the mixing model was applied to channel runoff and spring data sampled on 17 May 2012 and 11 April 2014.

4 Results

4.1 Streamflow response and variability of time of rise

Runoff in the monitored rock channels and stream sections shows a clear response to precipitation and snowmelt inputs (representative examples are shown in Fig. 2). Runoff at the outlet of ChA and ChB is not existent or negligible during the winter months and is present in spring and summer only after rainstorms or as consequence of snowmelt (approximately 25% of the summer monitoring time). On the contrary, winter baseflow at BCC and the outlet of RVC is low but continuous. Hydrograph analysis for the monitored years typically reveals more rapid recessions at ChA and ChB compared to BCC and particularly RVC but a large variability in the hydrograph shape depending on storm duration, storm size and snowmelt intensity was observed (Fig. 2)

There is a relatively low variability of times of rise for all identified rainfall, snowmelt and mixed rainfall-snowmelt events among the four catchments (Fig. 3). Although the non-parametric Kruskal-Wallis one-way analysis of variance reveals significant differences in the median values among the

1
2 313 four catchments ($p<0.001$ for snowmelt events and rainfall events, $p=0.006$ for mixed events), these
3
4 314 differences are overall limited for each type of event. Particularly, response times are statistically
5
6 315 identical for the two rock channels for all types of events (non-parametric Mann-Whitney test,
7
8 316 $p>>0.05$, median of 1.0 and 6.0 hours for rainfall and snowmelt events, respectively, for both
9
10 317 subcatchments, and median of 5.2 and 6.0 for mixed events for ChA and ChB, respectively) and
11
12 318 different compared to those of BCC and RVC. BCC shows the longest median times of rise and the
13
14 319 highest variability for rainfall and mixed events (median of 3.2 and 7.2 hours, respectively), and
15
16 320 RVC the longest median times of rise for snowmelt events (median of 7.5 hours). Overall, the
17
18 321 shortest times of rise are observed for rainfall events, especially for ChA and ChB.
19
20
21
22

23
24 323 **4.2 Tracer signature in different waters**

25
26 324 The variability in the isotopic composition and EC of all waters sampled in the study catchments is
27
28 325 large (Fig. 4). Rain and winter snow have similar low values of EC but contrasting isotopic
29
30 326 composition, with rain and winter snow having the most enriched and the most depleted median
31
32 327 isotopic composition in the entire dataset, respectively. The signature of snowmelt is more variable
33
34 328 and more enriched than winter snow but still more depleted than summer snow. However, the EC
35
36 329 values are similar. Spring water and channel runoff at ChA, ChB and upper RVC have noticeably
37
38 330 lower EC compared to BCC and RVC but more similar isotopic composition although much more
39
40 331 variable in the former sites. Shallow groundwater and soil water are the sources with the highest
41
42 332 variability in EC.
43
44
45

46 333
47
48 334 The tracer signature in the water sources sampled in the catchment shows a clear seasonal
49
50 335 variability (Fig. 5). As expected, isotopes in rainfall are characterized by the seasonal effect
51
52 336 (Rozanski et al., 1993), with more enriched values during warm months and vice versa, and
53
54 337 differences up to more than 40‰ (Fig. 5, top panel left). The isotopic composition of channel
55
56 338 runoff and spring water at ChA and ChB shows large temporal variations, with the most depleted
57
58
59
60

values observed during the spring melting. Channel runoff, spring water and shallow groundwater at BCC and lower RVC follow a similar pattern, although more damped and slightly temporally-shifted compared to that of precipitation (Fig. 5, left panels). The isotopic composition of shallow groundwater shows a similar temporal trend to those, well temporally correlated, of channel runoff at BCC and lower RVC and the corresponding springs but piezometer M26 presents a higher variability in $\delta^2\text{H}$ compared to piezometer P17. The seasonal trend in EC at ChA, ChB, BCC and lower RVC is less clear except for the two piezometers that typically show the lowest values in late spring-early summer (Fig. 5, right panels). Channel runoff at RVC has generally lower, more variable and not well temporally correlated EC compared to channel runoff at BCC. The temporal trend in EC is more similar between the BCC and lower RVC springs compared to channel runoff, with the BCC spring presenting consistently higher values than the lower RVC spring. EC fluctuations in M26 show a higher amplitude and overall much lower values compared to P17.

4.3 EMMA and dual isotope analysis

The combined tracer signature of rainfall, snowmelt, soil water and shallow groundwater defines a mixing space that comprises all samples of channel runoff and spring water (Fig. 6). Springs and channel runoff at BCC and in the lower RVC plot close to soil water and partially to shallow groundwater, whereas springs and channel runoff in ChA, ChB and the upper RCV plot closer to rainfall and snowmelt. Springs and channel runoff in ChA, ChB and the upper RCV span a wide range in the isotopic composition, approximately between -55‰ and -115‰ whereas their EC has a relatively small range, roughly between 90 $\mu\text{S}/\text{cm}$ and 190 $\mu\text{S}/\text{cm}$. On the contrary, springs and channel runoff at BCC and in the lower RVC show a much smaller variability in the isotopic composition, approximately between -80‰ and -100‰, and a larger EC range, roughly between 150 $\mu\text{S}/\text{cm}$ and 380 $\mu\text{S}/\text{cm}$. The only overlap between these two water groups is observed for some samples of channel runoff in the lower RVC during snowmelt periods.

1
2 365 The monthly-integrated rainfall samples collected over three seasons define a local meteoric water
3
4 366 line (LMWL) that has the same slope (8.0, or very close to it considering the uncertainty) as the
5
6 367 global meteoric water line (GMWL) but has a higher intercept (13.5‰ vs. 10.0‰) (Table III).
7
8 368 Unfortunately, fresh snow samples are not available and so the isotopic characterization of winter
9
10 369 precipitation is not possible.
11
12 370 Channel runoff and spring water at BCC and lower RVC show a narrower isotopic range compared
13
14 371 to that of ChA, ChB and upper RVC. However, the statistical comparison of the slopes of
15
16 372 regression lines indicate that both channel runoff groups have a slope equal to that of the LMWL.
17
18 373 More interestingly, the comparison of the slopes of regression lines reveals that the slope of
19
20 374 snowmelt samples is significantly different from that of spring water at BCC and lower RVC but
21
22 375 equal to that of spring water at ChA, ChB and upper RVC. Finally, shallow groundwater in P17 and
23
24 376 M26 plot well along the LMWL, have slope statistically equal to each other and to that of the
25
26 377 LMWL and significantly different from that of soil water samples that are more enriched and plot
27
28 378 partly below the LMWL (Table III).
29
30
31
32
33
34

35 380 **4.4 Two-component mixing model results**

36
37 381 The application of the two-component mixing model to spring water and channel runoff sampled in
38
39 382 the two rocky subcatchments on 5 July 2011 reveals different contributions of snowmelt (Fig. 7).
40
41 383 For springs SPR3, SPR4, SPR6 and SPR9, located in convex areas (Fig. 1), and for runoff sampled
42
43 384 at the outlet of ChA, snowmelt fractions vary in a small range (56% - 64%) with comparable
44
45 385 uncertainty values (between $\pm 8\%$ and $\pm 10\%$). However, for SPR2, located on the divide between
46
47 386 ChA and ChB, in a zone less prone to snow accumulation (Fig. 1), the snowmelt fraction is
48
49 387 remarkably lower and uncertainty much higher ($6\% \pm 21\%$). For other days later in the seasons when
50
51 388 spring water in the upper RVC and ChA was sampled (28 September 2012 and 5 September 2013)
52
53 389 the isotopic compositions of the springs (approximately between -62‰ and -65‰) was very similar
54
55 390 to that of precipitation (approximately between -67‰ and -70‰) and the application of the mixing
56
57
58
59
60

model was not possible (Klaus and McDonnell, 2013). The mixing model applied to data from BCC and the lower part of RVC for two dates highlights marked differences in the snowmelt contributions as well (Fig. 8). Snowmelt fractions in channel runoff and spring water during late spring (17 May 2012) were very low or negligible (Fig. 8, top panel) whereas snowmelt played a much more important role in forming channel runoff and spring water during mid-spring (11 April 2014, Fig. 8, bottom panel). All other samples taken at BCC and lower RVC during the study period for which the mixing model application was possible have been reported in a previous study (Penna et al., 2016).

5 Discussion

5.1 Controls on response times

The smaller variability in water stage values of ChA, especially, and ChB, and the occurrence of more similar maxima over the study years compared to the other two catchments (not shown) suggests that the rock channels follow relative quickly subsurface flow pathways and have a storage system that can be saturated more often and more rapidly than that of BCC and RVC. On the contrary, the runoff response of BCC and RVC is more sensitive to the intensity of individual water inputs, and the variability of streamflow response is particularly marked at BCC. These differences in runoff response reflect quite well the response timing of the four catchments (Fig. 3), with the same short times of rise for ChA and ChB and slightly longer times of rise for the other two catchments (especially longer for BCC during rainfall events). We relate this behaviour to the buffer effect produced by the greater soil cover area at BCC and RVC (and proportionally greater in BCC than RVC, Table I) compared to the two rock subcatchments, and the associated role of soil in regulating antecedent moisture conditions that can significantly affect the intensity (e.g., Penna et al., 2011; Nadal-Romero et al., in press) and the timing (Montgomery and Dietrich, 2002; Haga et al., 2005) of runoff response of soil-mantled catchments. Montgomery and Dietrich (2002) reported a weak correlation between catchment size, catchment slope and response time for the CB2

1
2 417 catchment in the Oregon Coast Range. Our data are too limited to perform a robust statistical
3
4 418 analysis but the poor relation that we found between average and median time of rise, catchment
5
6 419 slope and catchment area (not reported) let us hypothesize that other variables, such as the soil
7
8 420 cover, may have a greater influence on the runoff timing of the study catchment. Particularly, the
9
10 421 only slightly longer times of rise of RVC compared to the one order of magnitude smaller rocky
11
12 422 subcatchments, and only shorter times of rise at least for rainfall and mixed events compared to
13
14 423 BCC (Table I and Fig. 3) may be due to the compensating effects of fast response in subvertical
15
16 424 Dolomitic cliffs of the upper part of RVC and the delayed response in the soil-covered central and
17
18 425 lower part of the catchment. Moreover, the smaller difference in the median time of rise between
19
20 426 BCC and the two rocky subcatchments during snowmelt events compared to mixed events and,
21
22 427 especially, rainfall events can be due to the saturated conditions that BCC typically experiences
23
24 428 during the snowmelt period and that produce fast and marked streamflow response (Penna et al.,
25
26 429 2016).
27
28
29
30 430
31
32
33 431 The response times we found for the four study catchments are generally different from those
34
35 432 identified by other researchers in various small catchments worldwide, although the definition of
36
37 433 response time is not consistent with ours and therefore lag times are not directly comparable. For
38
39 434 instance, Onda et al. (2001) observed much longer response times for six catchments below 10 ha in
40
41 435 Japan whereas Talei et al. (2012) computed much shorter (< 1 hr) response times for a 0.65 ha
42
43 436 catchment in Singapore. Overall, the range of values identified for RVC and its subcatchments is
44
45 437 consistent with that reported by Montgomery and Dietrich (2002) for two unchanneled catchments
46
47 438 in the Oregon Coast Range, USA, although their catchments were one and two orders of magnitude
48
49 439 smaller than the ones presented in this study. These findings highlight the marked variability in lag
50
51 440 times and suggest that a combination of different processes controls the timing of runoff response in
52
53 441 catchments of different size, geological setting and morphometric characteristics.
54
55
56
57 442
58
59
60

5.2 Spatial and temporal variability of channel runoff, spring water and shallow groundwater

The noticeable variability in the isotopic composition and EC of all water sources sampled in this study (Fig. 4) reveals complex hydrochemical signatures and physical interactions between precipitation, surface waters and groundwater at RVC and its subcatchments, as recently observed in other high-elevation mountain catchments (Penna et al., 2014b; Fan et al., 2015; Fischer et al., 2015; Carturan et al., 2016). The lower EC in spring water and channel runoff at ChA, ChB and upper RVC suggests shorter contact with rocks and therefore faster water transmission compared to BCC and lower RVC, in agreement with shorter times of rise (Fig. 3). The isotopic composition of springs and channel runoff at BCC and RVC is little variable (Fig. 4) and relatively constant throughout the year, except during spring time when the observed depletion indicates the influence of snowmelt (Holko et al., 2013) (Fig. 5). This suggests the presence of a deeper flow component that facilitates the water-soil hydrochemical interactions leading to higher EC and damped isotope variability of channel runoff and springs compared to ChA and ChB. Moreover, the isotopic composition of the two springs is statistically identical to that of channel runoff at the BCC outlet (Penna et al., 2016) suggesting a similar origin and/or a connection between spring water and stream water in this subcatchment. On the contrary, the much higher isotopic variability of spring water and channel runoff at ChA, ChB and upper RVC overlapping more broadly with the isotopic signature of snowmelt than that of BCC and lower RVC, suggests a greater influence of snowmelt at those locations, consistently with their higher elevation. However, it must be considered that the different sample number and sampling times mainly during summer and not throughout the year as at BCC and lower RVC could affect this higher variability.

The highly seasonally variable isotopic composition and EC of shallow groundwater at BCC (Fig. 4), especially of M26 (more than 60‰ in $\delta^2\text{H}$ and 500 $\mu\text{S}/\text{cm}$, Fig. 5) that is quite different compared to that of P17 (Fig. 5), highlights the complex hydrochemical behaviour of groundwater even at the small spatial scale, indicating the need of further and more detailed investigations in this subcatchment.

1
2
3
4
5
6
7
8
9
10
11
12
13
14
15
16
17
18
19
20
21
22
23
24
25
26
27
28
29
30
31
32
33
34
35
36
37
38
39
40
41
42
43
44
45
46
47
48
49
50
51
52
53
54
55
56
57
58
59
60

5.3 Water origin and role of snowmelt

The mixing plot (Fig. 6) combining the isotopic composition and EC of all water samples indicates that rainfall, snowmelt, soil water and shallow groundwater act as end-members for channel runoff and spring recharge in the study area. However, given the limited spatial measurements of soil water and shallow groundwater, and the high variability of their response (Penna et al., 2015) and tracer signature (Penna et al., 2016) we cannot exclude that those sources are representative of a local situation affecting only the lower part of BCC but not significantly contributing to the main stream.

Summer snow samples have a $\delta^2\text{H}$ - $\delta^{18}\text{O}$ slope lower than 8 (Table III) revealing some kinetic fractionation due to sublimation/evaporation and/or isotopic exchange between liquid water and ice during the melting phase (Lee et al., 2010), whereas snowmelt samples taken in spring follow the LMWL (Table III) indicating negligible melt-freeze mass exchange between the solid and liquid phases during the snow metamorphism (Zhou et al., 2008). Despite these differences, the average and standard deviation of $\delta^2\text{H}$ and EC of summer snow plot entirely within the variability of snowmelt not allowing to distinguish summer snow as an individual end-member.

The position of ChA, ChB and RVC spring and channel runoff samples close to snowmelt and rainfall samples indicates a larger influence of these two end-members than for spring water and channel runoff at BCC and lower RVC which are more related to shallow groundwater and soil water (Fig. 6). This is reasonable considering the more limited distribution or even absence of soil cover in the upper part of the study catchment. The much larger range in $\delta^2\text{H}$ and smaller range in EC in spring and channel runoff samples at ChA, ChB and upper RVC corroborate this finding, because they reflect the influence of snowmelt and rainfall that show high variability in isotopic composition but low variability in EC, in contrast to BCC and lower RVC where spring and channel runoff samples reflect the high variability of soil water and shallow groundwater for both tracers. These results agree well with recent findings at BCC that revealed a dominant contribution of pre-

event water (assumed to be a mixture of shallow groundwater and soil water) to streamflow during both rainfall- and snowmelt-runoff events (Penna et al., 2016). Furthermore, the significantly different $\delta^2\text{H}$ - $\delta^{18}\text{O}$ slope of snowmelt samples with respect to that of spring water at BCC and lower RVC but equal to that of spring water at ChA, ChB and upper RVC indicates a stronger linkage and a more direct influence of snowmelt on spring water in the upper part than in the lower part of the study catchment. The only connection between these two seemingly decoupled water systems is provided by the main stream which partially transfers downstream water inputs from the upper catchment and partly receives contributions from the lateral tributaries in the lower catchment, resulting in the tracer signature of samples from the lower RVC overlapping with that of channel runoff in ChA, ChB and BCC, especially during snowmelt periods (Fig. 6).

The importance of snowpack meltwater for groundwater recharge in the upper RVC is stressed by the high computed fractions of snowmelt in spring water (Fig. 7). Although these fractions refer to one sampling day only and analyses on a more extended dataset would be advisable, they are generally higher than the isotope-based proportions of snowmelt in spring water calculated for other high-elevation catchments in South-Western USA and Himalaya (Earman et al., 2006; Jeelani et al., 2010) and only slightly lower than those computed for a glacierized catchment in South Tyrol, Northern Italy (Penna et al., 2014b). The snowmelt fractions computed for ChA (Fig. 7) are much higher and slightly higher than those found in late and mid-spring, respectively, for channel runoff and spring water at BCC and RVC in the proximity of the outlet (Fig. 8). Interestingly, the snowmelt fraction observed in ChA is also noticeably higher, even considering uncertainty, than the average and maximum snowmelt fractions observed at the BCC outlet during six melt-induced runoff events in 2010, 2011 and 2012 (Penna et al., 2016), underlining the more relevant role of snowmelt on spring water and channel runoff in the upper than lower part of RVC.

5.4. Main limitations of the study

1
2 521 Despite the efforts played in the field by our group during the monitoring years, there are intrinsic
3
4 522 limitations in this research that are mainly associated with the complexity of sampling waters in
5
6 523 environments at high elevation and difficult accessibility, and that should be mentioned.
7
8 524 Particularly, the monthly temporal resolution of sample collection in the upper part of the RVC can
9
10 525 mask some variability in the tracer signature of water sources and hamper a more detailed
11
12 526 understanding of the end-member temporal dynamics. Furthermore, a more even distribution of
13
14 527 sampling locations along the main stream is advisable in order to detect relevant spatial changes in
15
16 528 EC and isotopic composition due to lateral subsurface contributions. Additionally, more locations
17
18 529 for soil water sampling are necessary in order to take into account the expected marked spatial
19
20 530 variability of the tracer signature of the unsaturated zone in the soil-mantled portion of the
21
22 531 catchment, and specifically in different landscape zones (e.g., riparian zone, hillslopes).
23
24 532 Particularly, this issue has been addressed by our group sampling water sources, including soil
25
26 533 water at different locations, at high temporal resolution for multiple tracers during different melt-
27
28 534 induced runoff events at BCC in the 2016 snowmelt season (unpublished results).
29
30
31
32
33
34

35 536 **6 Conclusions**

36
37 537 The analysis of rainfall and channel hydrometric data coupled with environmental tracers sampled
38
39 538 at different locations and elevations in the steep nested Rio Vauz Catchment (Eastern Italian Alps)
40
41 539 allowed us to gain new insights into the timing of hydrological response at different spatial scales
42
43 540 and the main water sources influencing spring recharge and channel runoff formation in Dolomitic
44
45 541 headwater catchments as well as to make advancement in the comprehension of water flow
46
47 542 pathways in these environments. As far as we know, this is the first experimental tracer-based study
48
49 543 addressing these issues in a snowmelt-dominated mountain catchment featuring a marked elevation
50
51 544 gradient.
52
53
54 545 The two monitored rocky subcatchments in the upper RVC show overall shorter response times
55
56 546 compared to the soil-mantled subcatchment and the catchment as a whole but differences in the
57
58
59
60

1
2 547 computed times of rise are small and appear to be mainly related to the land cover (soil mantled vs.
3
4 548 bare rock) and the associated hydrological processes. The high density of structural discontinuities
5
6 549 associated to fractures and stratification and the presence of karstic features where water can
7
8 550 infiltrate and reside, as well as the presence of a low-slope belt in the intermediate part of these
9
10 551 subcatchments, affect the hydrological response time of the channels laying at the base of the
11
12 552 subvertical Dolomitic cliffs, making it longer than the one expected on impervious bare rocks but
13
14 553 still faster than that of the monitored soil-mantled subcatchment. The large variability in the
15
16 554 isotopic composition and EC of several water sources sampled in various years reflects the
17
18 555 geological and geomorphological complexity of the study area. Our tracer results indicate rainfall,
19
20 556 snowmelt, shallow groundwater and soil water as the principal end-members for channel runoff
21
22 557 formation and spring recharge, although shallow groundwater and soil water might have a local
23
24 558 influence. Particularly, the end-member mixing analysis and the dual isotope approach suggest that
25
26 559 elevation and land cover affect the relative importance of these end-members in the various portions
27
28 560 of RVC, with soil water and shallow groundwater dominating in the soil-mantled BCC and rainfall
29
30 561 and snowmelt influencing more directly runoff and spring water in the rocky ChA and ChB
31
32 562 subcatchments. Current hydrometric and tracer results combined with previous investigations in the
33
34 563 study area reveal a complex pattern of hydrological connectivity and let us develop a preliminary
35
36 564 conceptual model of water transmission at RVC. This is important because it can be applied and/or
37
38 565 compared to other mountain catchments characterized by strong elevation gradients. The nested
39
40 566 catchment organization reflects the geological structure and supports the hypothesis of the presence
41
42 567 of two water circulation systems, hydrologically connected through the main channel but
43
44 568 characterized by different response times and tracer signature. The low EC and the high variability
45
46 569 of the isotopic composition of channel runoff and spring water in the two rocky subcatchments and
47
48 570 upper RVC, as well as the shorter response times than in BCC and lower RVC, indicate a poor
49
50 571 hydrochemical interaction between infiltrating rainfall and snowmelt and soil and/or rocks, and
51
52 572 limited and relatively fast subsurface flow pathways. Snowmelt is particularly important for the
53
54
55
56
57
58
59
60

1
2 573 springs localized in hollows and rainfall is more relevant for springs located on ridges, less prone to
3
4 574 snow accumulation. On the contrary, rainfall and snowmelt infiltrate and are likely stored for longer
5
6 575 times in the soil and subsoil of BCC and the lower part of RVC, contributing to recharge the
7
8 576 unsaturated and shallow groundwater and representing important sources for baseflow and spring
9
10 577 water. Here, the possible presence of a deep and slow subsurface flow component, related to the
11
12 578 larger aquifer mainly corresponding to the “Dolomia Cassiana” formation, damps the timing of the
13
14 579 hydrological response and leads to stronger hydrochemical interactions between water and soil,
15
16 580 resulting in higher EC and reduced variability of the isotopic composition of channel runoff and
17
18 581 springs. The influence of snowmelt is smaller and limited to intense snowmelt periods, whereas
19
20 582 rainfall contributes most to channel runoff during intense rainfall events with wet antecedent
21
22 583 conditions, due to overland flow on expanded saturated areas, especially in the small lateral
23
24 584 tributaries draining into the lower part of the main stream.
25
26
27
28 585 These experimental results allowed us to obtain a preliminary overview of response times, water
29
30 586 origin and transmission across this steep Dolomitic catchment. However, more detailed analyses
31
32 587 from different perspectives are necessary in order to better understand the complex hydrogeological
33
34 588 interplays that determine the connectivity network and regulate water flow in these aquifers. For
35
36 589 instance, the application of multiple tracers (e.g., stable and unstable isotopes of water, major
37
38 590 anions and cations, silica, radon etc.) at high frequency during specific field campaigns coupled
39
40 591 with hydrogeological analyses can open new ways to conceptualize and interpret storage and
41
42 592 movements of surface and subsurface water in partly karst mountain catchments featuring strong
43
44 593 elevation gradients.
45
46
47
48
49

50
51 595 **Acknowledgements**

52
53 596 The research was partly supported by the grant “Bando 2014 per il finanziamento di attrezzature
54
55 597 scientifiche finalizzate alla ricerca” (University of Padova) and by the DIBA NextData Project
56
57 598 (Italian Ministry of University and Research). We thank many undergraduate, graduate and PhD
58
59
60

1
2 599 students who contributed to field work. The Agency for Environmental Protection of Veneto
3
4 600 Region (ARPAV) is acknowledged for the meteorological data and logistical support.
5
6 601
7
8
9
10
11
12
13
14
15
16
17
18
19
20
21
22
23
24
25
26
27
28
29
30
31
32
33
34
35
36
37
38
39
40
41
42
43
44
45
46
47
48
49
50
51
52
53
54
55
56
57
58
59
60

For Peer Review

1
2
3
4
5
6
7
8
9
10
11
12
13
14
15
16
17
18
19
20
21
22
23
24
25
26
27
28
29
30
31
32
33
34
35
36
37
38
39
40
41
42
43
44
45
46
47
48
49
50
51
52
53
54
55
56
57
58
59
60

References

Beniston, M., 1997. Variations of snow depth and duration in the Swiss Alps over the last 50 years: links to changes in large-scale climatic forcings, *Climatic Change*, 36, 281, 300. doi: 10.1023/A:1005310214361

Bishop, K., Buffam, I., Erlandsson, M., Fölster, J., Laudon, H., Seibert, J., Temnerud, J., 2008. *Aqua Incognita: the unknown headwaters*. *Hydrological Processes* 22, 1239–1242. doi:10.1002/hyp.7049

Böckli, L., Brenning, A., Gruber, S., Noetzli, J., 2012. Permafrost distribution in the European Alps: Calculation and evaluation of an index map and summary statistics. *The Cryosphere*, 6, 807-820. doi:10.5194/tc-6-807-2012, 2012.

Bosellini, A., Gianolla, P., Stefani, M., 2003. Geology of the Dolomites, *Episodes*, 26, 181-185.

Camporese, M., Penna, D., Borga, M., Paniconi, C., 2014. A field and modeling study of nonlinear storage-discharge dynamics for an Alpine headwater catchment: nonlinear storage-discharge dynamics of an alpine catchment. *Water Resources Research* 50, 806–822. doi:10.1002/2013WR013604

Carturan, L., Zuecco, G., Seppi, R., Zanoner, T., Borga, M., Carton, A., Dalla Fontana, G., 2016. Catchment-scale permafrost mapping using spring water characteristics. *Permafrost and Periglacial Processes*, 27, 253-270. doi: 10.1002/ppp.1875

Dahlke, H.E., Lyon, S.W., Jansson, P., Karlin, T., Rosqvist, G., 2014. Isotopic investigation of runoff generation in a glacierized catchment in northern Sweden: isotopic investigation of runoff generation in a glacierized catchment. *Hydrological Processes* 28, 1383–1398. doi:10.1002/hyp.9668

Dingman, S. L., 2002. *Physical Hydrology*, second edition. Prentice Hall, 2002.

Doglioni, C., Carminati, E., 2008. *Structural Styles & Dolomites Field Trip*. *Memorie Descrittive della Carta Geologica d'Italia*, vol. 82, pp. 1-293.

- 627 Earman, S., Campbell, A.R., Phillips, F.M., Newman, B.D., 2006. Isotopic exchange between snow
628 and atmospheric water vapor: Estimation of the snowmelt component of groundwater recharge
629 in the southwestern United States. *Journal of Geophysical Research* 111.
630 doi:10.1029/2005JD006470
- 631 Engel, M., Penna, D., Bertoldi, G., Dell'Agnese, A., Soulsby, C., Comiti, F., 2016. Identifying run-
632 off contributions during melt-induced run-off events in a glacierized alpine catchment.
633 *Hydrological Processes*, 30, 343-364. doi:10.1002/hyp.10577
- 634 Fan, Y., Chen, Y., Li, X., Li, W., Li, Q., 2015. Characteristics of water isotopes and ice-snowmelt
635 quantification in the Tizinafu River, north Kunlun Mountains, Central Asia. *Quaternary*
636 *International* 380-381, 116–122. doi:10.1016/j.quaint.2014.05.020
- 637 Fischer, B.M.C., Rinderer, M., Schneider, P., Ewen, T., Seibert, J., 2015. Contributing sources to
638 baseflow in pre-alpine headwaters using spatial snapshot sampling. *Hydrological Processes*, 29
639 (26), 5321-5336. doi:10.1002/hyp.10529
- 640 Genereux D., 1998. Quantifying uncertainty in tracer-based hydrograph separations. *Water*
641 *Resources Research*, 34(4), 915–919. doi:10.1029/98WR00010.
- 642 Haga, H., Matsumoto, Y., Matsutani, J., Fujita, M., Nishida, K., Sakamoto, Y., 2005. Flow paths,
643 rainfall properties, and antecedent soil moisture controlling lags to peak discharge in a granitic
644 unchanneled catchment. *Water Resources Research* 41, 41, W12410.
645 doi:10.1029/2005WR004236
- 646 Holko, L., Danko, M., Dóša, M., Kostka Z., Šanda M., Pfister L., Iffly, J.F., 2013. Spatial and
647 temporal variability of stable water isotopes in snow related hydrological processes. *Die*
648 *Bodenkultur* 39, 64 (3–4).
- 649 Howell, D. C., 2010. *Statistical methods for psychology* (7th ed.). Wadsworth, Cengage Learning,
650 Charles.

- 651 Jeelani, G., Bhat, N.A., Shivanna, K., 2010. Use of $\delta^{18}\text{O}$ tracer to identify stream and spring origins
652 of a mountainous catchment: A case study from Liddar watershed, Western Himalaya, India.
653 *Journal of Hydrology* 393, 257–264. doi:10.1016/j.jhydrol.2010.08.021
- 654 Jeelani, G., Saravana Kumar, U., Kumar, B., 2013. Variation of $\delta^{18}\text{O}$ and δD in precipitation and
655 stream waters across the Kashmir Himalaya (India) to distinguish and estimate the seasonal
656 sources of stream flow. *Journal of Hydrology* 481, 157–165. doi:10.1016/j.jhydrol.2012.12.035
- 657 Jin, L., Siegel, D.I., Lautz, L.K., Lu, Z., 2012. Identifying streamflow sources during spring
658 snowmelt using water chemistry and isotopic composition in semi-arid mountain streams.
659 *Journal of Hydrology* 470–471, 289–301. doi:10.1016/j.jhydrol.2012.09.009
- 660 Klaus, J., McDonnell, J.J., 2013. Hydrograph separation using stable isotopes: Review and
661 evaluation. *Journal of Hydrology* 505, 47–64. doi:10.1016/j.jhydrol.2013.09.006
- 662 Klaus, J., McDonnell, J.J., Jackson, C.R., Du, E., Griffiths, N.A., 2015. Where does streamwater
663 come from in low-relief forested watersheds? A dual-isotope approach. *Hydrology and Earth
664 System Sciences* 19, 125–135. doi:10.5194/hess-19-125-2015
- 665 Knowles, J.F., Harpold, A.A., Cowie, R., Zeff, M., Barnard, H.R., Burns, S.P., Blanken, P.D.,
666 Morse, J.F., Williams, M.W., 2015. The relative contributions of alpine and subalpine
667 ecosystems to the water balance of a mountainous, headwater catchment. *Hydrological
668 Processes* 29, 4794–4808. doi:10.1002/hyp.10526
- 669 Krainer, K., Mussner, L., Behm, M., Hausmann, H., 2012. Multi-disciplinary investigation of an
670 active rock glacier in the Sella Group (Dolomites; Northern Italy). *Austrian Journal of Earth
671 Sciences* 105, 48–62.
- 672 Lee, J., Feng, X., Faiia, A., Faiia, A. M., Posmentier, E. S., Kirchner, J. W., Osterhuber, R., Taylor,
673 S., 2010. Isotopic evolution of a seasonal snowcover and its melt by isotopic exchange between
674 liquid water and ice. *Chemical Geology* 270, 126–134. doi: 10.1016/j.chemgeo.2009.11.011.

- 675 Liu, F., Hunsaker, C., Bales, R.C., 2013. Controls of streamflow generation in small catchments
676 across the snow-rain transition in the Southern Sierra Nevada, California. *Hydrological*
677 *Processes* 27, 1959–1972. doi:10.1002/hyp.9304
- 678 Liu, F., Song, X., Yang, L., Zhang, Y., Han, D., Ma, Y., Bu, H., 2015. Identifying the origin and
679 geochemical evolution of groundwater using hydrochemistry and stable isotopes in the Subei
680 Lake basin, Ordos energy base, Northwestern China. *Hydrology and Earth System Sciences* 19,
681 551–565. doi:10.5194/hess-19-551-2015
- 682 Liu, Z., Yao, Z.. Contribution of glacial melt to river runoff as determined by stable isotopes at the
683 source region of the Yangtze River, China. *Hydrology Research* nh2015089, in press.
684 doi:10.2166/nh.2015.089
- 685 Lundquist, J.D., Dettinger, M.D., Cayan, D.R., 2005. Snow-fed streamflow timing at different basin
686 scales: Case study of the Tuolumne River above Hetch Hetchy, Yosemite, California. *Water*
687 *Resources Research* 41, W07005. doi:10.1029/2004WR003933.
- 688 Mair, V., Zischg, A., Lang, K., Tonidandel, D., Krainer, K., Kellerer-Pirklbauer, A., Deline, P.,
689 Schoeneich, P., Cremonese, E., Pogliotti, P., Gruber, S., Böckli, L., 2011. PermaNET -
690 Permafrost Long-term Monitoring Network. Synthesis report. *INTERPRAEVENT Journal*
691 *series 1, Report 3. Klagenfurt.*
- 692 Marchi, L., Dalla Fontana, G., Cavalli, M., Tagliavini, F., 2008. Rocky headwaters in the
693 Dolomites, Italy: field observations and topographic analysis. *Arctic, Antarctic, and Alpine*
694 *Research*, 40 (4), 685-694. doi: 10.1657/1523-0430(07-037)
- 695 Marchi, L., Cavalli, M., Trevisani, S. 2015. Hypsometric analysis of headwater rock basins in the
696 Dolomites (Eastern Alps) using high-resolution topography. *Geografiska Annaler, Series A:*
697 *Physical Geography*, 97, 2, 317-335. doi: 10.1111/geoa.12067
- 698 Maurya, A.S., Shah, M., Deshpande, R.D., Bhardwaj, R.M., Prasad, A., Gupta, S.K., 2011.
699 Hydrograph separation and precipitation source identification using stable water isotopes and

1
2 700 conductivity: River Ganga at Himalayan foothills. *Hydrological Processes* 25, 1521–1530.
3
4 701 doi:10.1002/hyp.7912
5
6 702 McGlynn, B.L., McDonnell, J.J., Seibert, J., Kendall, C., 2004. Scale effects on headwater
7
8 703 catchment runoff timing, flow sources, and groundwater-streamflow relations. *Water Resources*
9
10 704 Research 40, W07504. doi:10.1029/2003WR002494
11
12 705 Meng, Y., Liu, G., Li, M., 2015. Tracing the Sources and Processes of Groundwater in an Alpine
13
14 706 Glacierized Region in Southwest China: Evidence from Environmental Isotopes. *Water* 7,
15
16 707 2673–2690. doi:10.3390/w7062673
17
18 708 Meyles, E., Williams, A., Ternan, L., Dowd, J., 2003. Runoff generation in relation to soil moisture
19
20 709 patterns in a small Dartmoor catchment, Southwest England. *Hydrological Processes* 17, 251–
21
22 710 264. doi:10.1002/hyp.1122
23
24 711 Montgomery, D.R., Dietrich, W.E., 2002. Runoff generation in a steep, soil-mantled landscape.
25
26 712 *Water Resources Research* 38, 7–1–7–8. doi:10.1029/2001WR000822
27
28 713 Mueller M. H., Alaoui A., Alewell C.. Water and solute dynamics during rainfall events in
29
30 714 headwater catchments in the Central Swiss Alps under the influence of green alder shrubs and
31
32 715 wetland soils. *Ecohydrology*, in press. doi: 10.1002/eco.1692
33
34 716 Nadal-Romero, E., Cammeraat, E., Serrano-Muela, M.P., Lana-Renault, N., Regüés, D..
35
36 717 Hydrological response of an afforested catchment in a Mediterranean humid mountain area: a
37
38 718 comparative study with a natural forest. *Hydrological Processes*, in press.
39
40 719 doi:10.1002/hyp.10820
41
42 720 Ohlanders, N., Rodriguez, M., McPhee, J., 2013. Stable water isotope variation in a Central Andean
43
44 721 watershed dominated by glacier and snowmelt. *Hydrology and Earth System Sciences* 17,
45
46 722 1035–1050. doi:10.5194/hess-17-1035-2013
47
48 723 Onda, Y., Komatsu, Y., Tsujimura, M., Fujihara, J., 2001. The role of subsurface runoff through
49
50 724 bedrock on storm flow generation. *Hydrological Processes* 15, 1693–1706.
51
52 725 doi:10.1002/hyp.234
53
54
55
56
57
58
59
60

- Payn, R.A., Gooseff, M.N., McGlynn, B.L., Bencala, K.E., Wondzell, S.M., 2012. Exploring changes in the spatial distribution of stream baseflow generation during a seasonal recession. *Water Resources Research* 48, W04519. doi:10.1029/2011WR011552.
- Penna, D., Ahmad, M., Birks, S.J., Bouchaou, L., Brenčič, M., Butt, S., Holko, L., Jeelani, G., Martínez, D.E., Melikadze, G., Shanley, J.B., Sokratov, S.A., Stadnyk, T., Sugimoto, A., Vreča, P., 2014a. A new method of snowmelt sampling for water stable isotopes: scientific briefing. *Hydrological Processes* 28, 5637–5644. doi:10.1002/hyp.10273
- Penna, D., Engel, M., Mao, L., Dell’Agnese, A., Bertoldi, G., Comiti, F., 2014b. Tracer-based analysis of spatial and temporal variations of water sources in a glacierized catchment. *Hydrology and Earth System Sciences* 18, 5271–5288. doi:10.5194/hess-18-5271-2014
- Penna, D., Brocca, L., Borga, M., Dalla Fontana, G., 2013. Soil moisture temporal stability at different depths on two alpine hillslopes during wet and dry periods. *Journal of Hydrology* 477, 55–71. doi:10.1016/j.jhydrol.2012.10.052
- Penna, D., Mantese, N., Hopp, L., Dalla Fontana, G., Borga, M., 2015. Spatio-temporal variability of piezometric response on two steep alpine hillslopes. *Hydrological Processes* 29, 198–211. doi:10.1002/hyp.10140
- Penna, D., Stenni, B., Šanda, M., Wrede, S., Bogaard, T.A., Gobbi, A., Borga, M., Fischer, B.M.C., Bonazza, M., Chárová, Z., 2010. On the reproducibility and repeatability of laser absorption spectroscopy measurements for $\delta^2\text{H}$ and $\delta^{18}\text{O}$ isotopic analysis. *Hydrology and Earth System Sciences* 14, 1551–1566. doi:10.5194/hess-14-1551-2010
- Penna, D., Stenni, B., Šanda, M., Wrede, S., Bogaard, T.A., Michelini, M., Fischer, B.M.C., Gobbi, A., Mantese, N., Zuecco, G., Borga, M., Bonazza, M., Sobotková, M., Čejková, B., Wassenaar, L.I., 2012. Technical Note: Evaluation of between-sample memory effects in the analysis of $\delta^2\text{H}$ and $\delta^{18}\text{O}$ of water samples measured by laser spectrometers. *Hydrology and Earth System Sciences* 16, 3925–3933. doi:10.5194/hess-16-3925-2012

1
2 751 Penna, D., Tromp-van Meerveld, H.J., Gobbi, A., Borga, M., Dalla Fontana, G., 2011. The
3
4 752 influence of soil moisture on threshold runoff generation processes in an alpine headwater
5
6 753 catchment. *Hydrology and Earth System Sciences* 15, 689–702. doi:10.5194/hess-15-689-2011
7
8 754 Penna, D., van Meerveld, H.J., Zuecco, G., Dalla Fontana, G., Borga, M., 2016. Hydrological
9
10 755 response of an Alpine catchment to rainfall and snowmelt events. *Journal of Hydrology* 537,
11
12 756 382–397. doi:10.1016/j.jhydrol.2016.03.040
13
14
15 757 Pinder G. F., Jones J. F., 1969. Determination of ground-water component of peak discharge from
16
17 758 chemistry of total runoff. *Water Resources Research*, 5(2), 438–445, doi:
18
19 759 84110.1029/WR005i002p00438.
20
21 760 Rozanski, K., L. Araguas-Araguas, R. Gonfiantini, 1993. Isotopic Patterns in Modern Global
22
23 761 Precipitation, in *Climate Change in Continental Isotopic Records*, Geophysical Monograph 78,
24
25 762 p.1-36, American Geophysical Union.
26
27 763 Šanda, M., Vitvar, T., Kulasová, A., Jankovec, J., Císlarová, M., 2014. Run-off formation in a
28
29 764 humid, temperate headwater catchment using a combined hydrological, hydrochemical and
30
31 765 isotopic approach (Jizera Mountains, Czech Republic). *Hydrological Processes* 28, 3217–3229.
32
33 766 doi:10.1002/hyp.9847
34
35
36 767 Sando, R., Blasch, K.W., 2015. Predicting alpine headwater stream intermittency: a case study in
37
38 768 the northern Rocky Mountains. *Ecohydrology and Hydrobiology* 15, 68–80.
39
40 769 doi:10.1016/j.ecohyd.2015.04.002
41
42
43 770 Sidle, R. C., Tsuboyama, Y., Noguchi, S., Hosoda, I., Fujieda, M., Shimizu, T., 2000. Stormflow
44
45 771 generation in steep forested headwaters: a linked hydrogeomorphic paradigm. *Hydrological*
46
47 772 *Processes*, 14, 369–385. doi: 10.1002/(SICI)1099-1085(20000228)14:3<369::AID-
48
49 773 HYP943>3.0.CO;2-P
50
51
52 774 Sklash M. G., Farvolden R. N., 1979. Role of groundwater in storm runoff. *Journal of Hydrology*,
53
54 775 862 43(1–4), 45–65, doi: 10.1016/0022-1694(79)90164-1.
55
56
57
58
59
60

- 1
2 776 Talei, A., Chua, L.H.C., 2012. Influence of lag time on event-based rainfall–runoff modeling using
3
4 777 the data driven approach. *Journal of Hydrology* 438–439, 223–233.
5
6 778 doi:10.1016/j.jhydrol.2012.03.027
7
8 779 Uchida, T., Ken ichirou, K., Mizuyama, T., 2001. Effects of pipeflow on hydrological process and
9
10 780 its relation to landslide: a review of pipeflow studies in forested headwater catchments.
11
12 781 *Hydrological Processes* 15, 2151–2174. doi:10.1002/hyp.281
13
14 782 Williams P., Ford D., 2007. *Karst hydrogeology and Geomorphology*. John Wiley & Sons Ltd,
15
16 783 Chichester, England, 562 pp., ISBN: 978-0-470-84997-2.c
17
18 784 Wipfli, M.S., Richardson, J.S., Naiman, R.J., 2007. Ecological linkages between headwaters and
19
20 785 downstream ecosystems: transport of organic matter, invertebrates, and wood down headwater
21
22 786 channels. *Journal of the American Water Resources Association*, 43, 72–85. doi:
23
24 787 10.1111/j.1752-1688.2007.00007.x
25
26 788 Zhou, S., Nakawo, M., Hashimoto, S., Sakai, A., 2008. The effect of refreezing on the isotopic
27
28 789 composition of melting snowpack. *Hydrological Processes* 22, 873–882. doi:10.1002/hyp.6662
29
30
31
32
33
34
35
36
37
38
39
40
41
42
43
44
45
46
47
48
49
50
51
52
53
54
55
56
57
58
59
60

Tables

Table I. Basic properties of the study catchments.

	ChA	ChB	BCC	RVC
Area (km ²)	0.10	0.10	0.14	1.9
Elevation range (m a.s.l.)	2657-3131	2647-3152	1932-2515	1844-3152
Mean elevation (m a.s.l.)	2907	2930	2121	2408
Mean slope (°)	36.6	40.9	31.4	37.4
Lithology	“Dolomia Principale”		“Dolomia Cassiana” and “San Cassiano”	complex (see text)
Main land cover	Rock		grassland	rock, grassland, sparse trees
Soil cover	< 1%		93%	51%

Table II. Criteria for the identification of rainfall, snowmelt and mixed rainfall+snowmelt events.

Antecedent rainfall refers to rainfall data recorded within 5 hours prior to the flow peak at the weather station closest to each subcatchment.

Type of event	Snowmelt period	Antecedent rainfall
Rainfall	outside	> 1 mm
Snowmelt	within	< 1 mm
Rainfall+snowmelt	within	> 1 mm

Table III. Results of the linear regression for all isotope data for the different water sources. The standard error of the parameters of the linear regression is given in parentheses. All linear regressions are significant with $p < 0.001$.

	n	Slope	Intercept	R²	Sampling period
Rain (LMWL)	61	8.0 (± 0.1)	13.5 (± 1.4)	0.983	May–early–November 2011–2015
Snow (summer)	13	7.0 (± 0.6)	-9.7 (± 7.7)	0.935	June–September 2011–2013
Snow (spring + winter)	33	6.7 (± 0.3)	-12.4 (± 6.0)	0.930	February–April 2012–2015
Snowmelt	106	8.3 (± 0.1)	13.4 (± 1.8)	0.981	March 2010–April 2014
Channel runoff (BCC + RVC below 2500 m a.s.l.)	91	7.4 (± 0.3)	3.6 (± 3.5)	0.892	April 2010–October 2015 (all year round)
Channel runoff (ChA + ChB + RVC above 2500 m a.s.l.)	25	8.1 (± 0.2)	10.7 (± 2.8)	0.984	Early July–mid–October 2011–2013
Springs (BCC + RVC below 2500 m a.s.l.)	256	6.8 (± 0.2)	-4.6 (± 3.1)	0.750	April 2010–October 2015 (all year round)
Springs (ChA + ChB + RVC above 2500 m a.s.l.)	32	8.3 (± 0.3)	13.3 (± 3.1)	0.972	Early July–mid–October 2011–2013
Shallow groundwater (P17)	33	7.6 (± 0.4)	5.6 (± 5.4)	0.907	May 2012–October 2015 (all year round)
Shallow groundwater (M26)	25	7.7 (± 0.3)	7.4 (± 3.1)	0.975	May 2012–November 2014 (all year round)
Soil water	16	5.3 (± 0.6)	-18.4 (± 5.9)	0.845	June–November 2012–2015

1
2
3
4
5
6
7
8
9
10
11
12
13
14
15
16
17
18
19
20
21
22
23
24
25
26
27
28
29
30
31
32
33
34
35
36
37
38
39
40
41
42
43
44
45
46
47
48
49
50
51
52
53
54
55
56
57
58
59
60

Figures

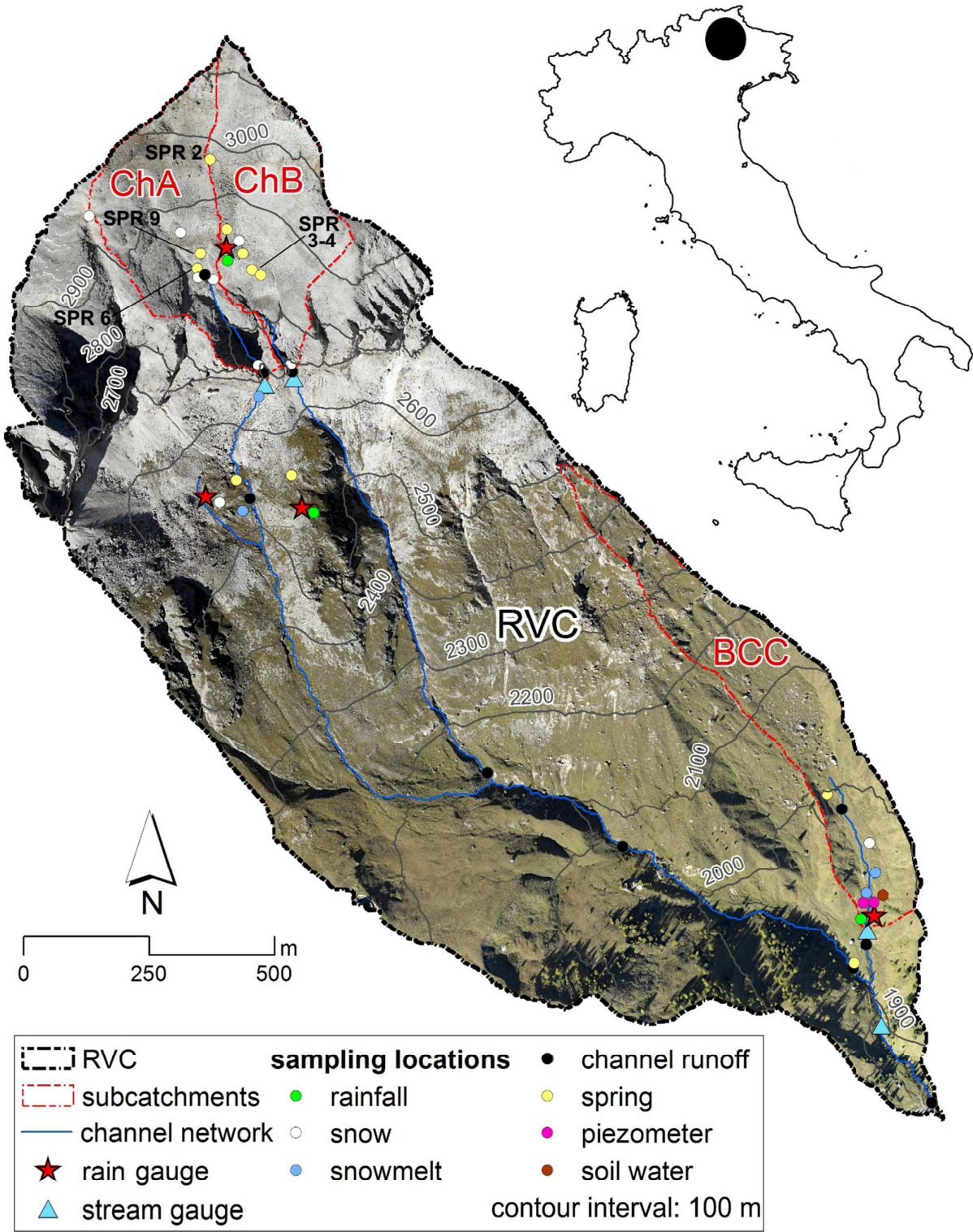


Fig. 1. Rio Vauz Catchment and its selected subcatchments with position of field instruments and sampling locations, and localization in Italy. The springs in the upper part of the catchment for which the two-component mixing model was applied (see Fig. 7) are labelled.

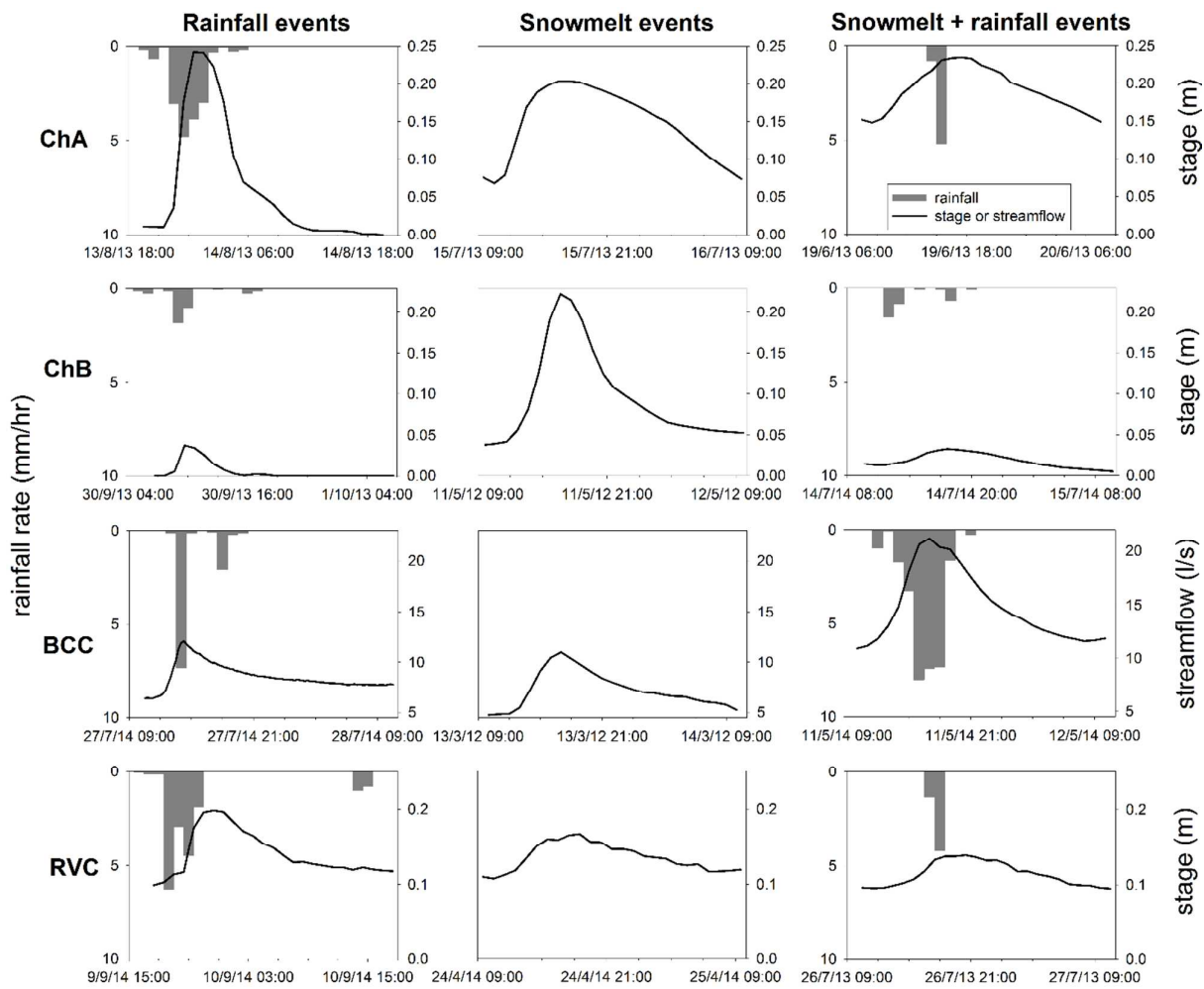


Fig. 2. Examples of rainfall-runoff events, snowmelt-runoff events and mixed-runoff events for all study catchments.

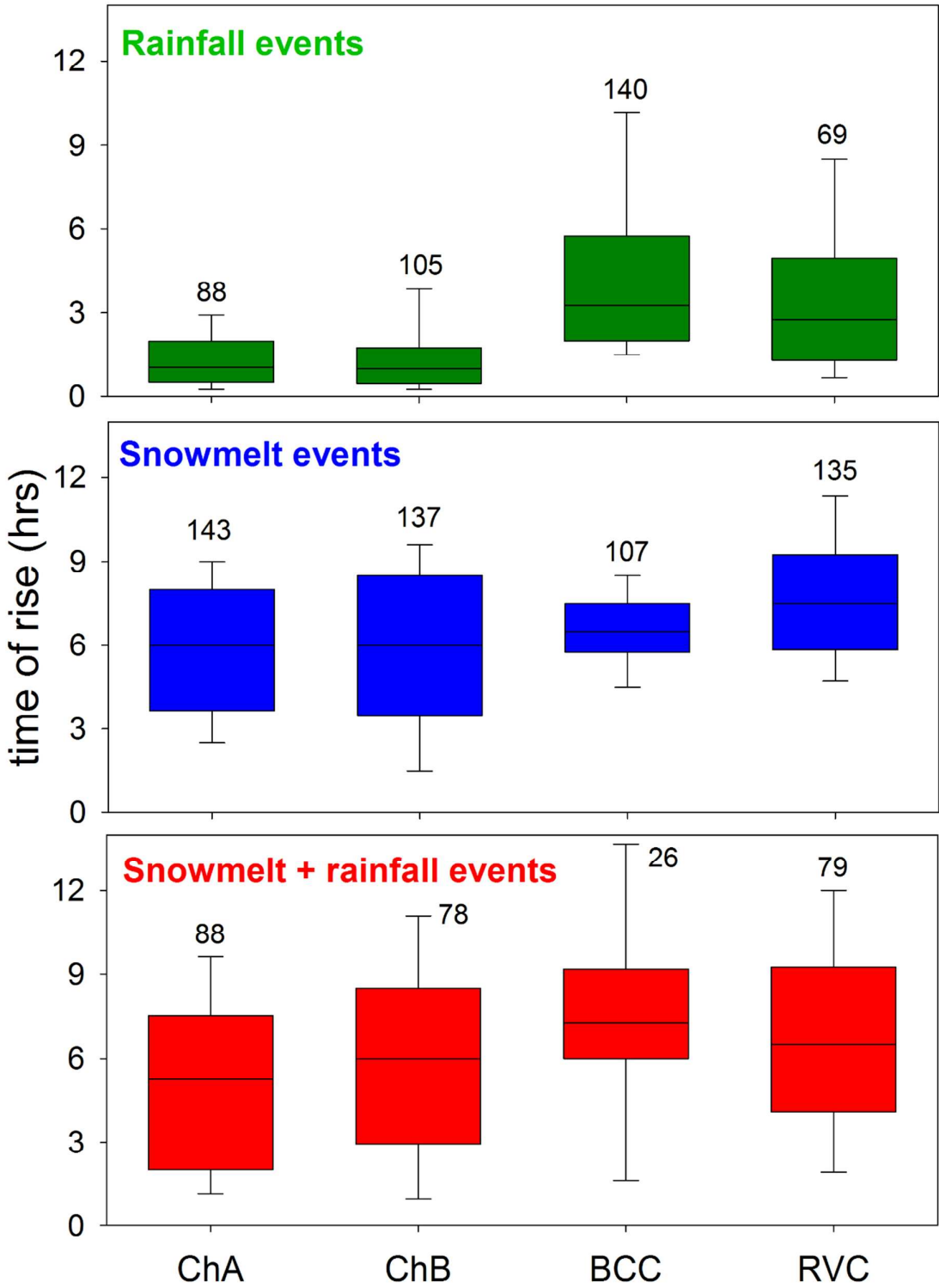


Fig. 3. Box-plot of time of rise for rainfall, snowmelt, and mixed snowmelt-rainfall events for the four study catchments. The numbers above or close to each box indicate the sample size. The boxes indicate the 25th and 75th percentile, the whiskers indicate the 10th and 90th percentile, the horizontal line within the box marks the median.

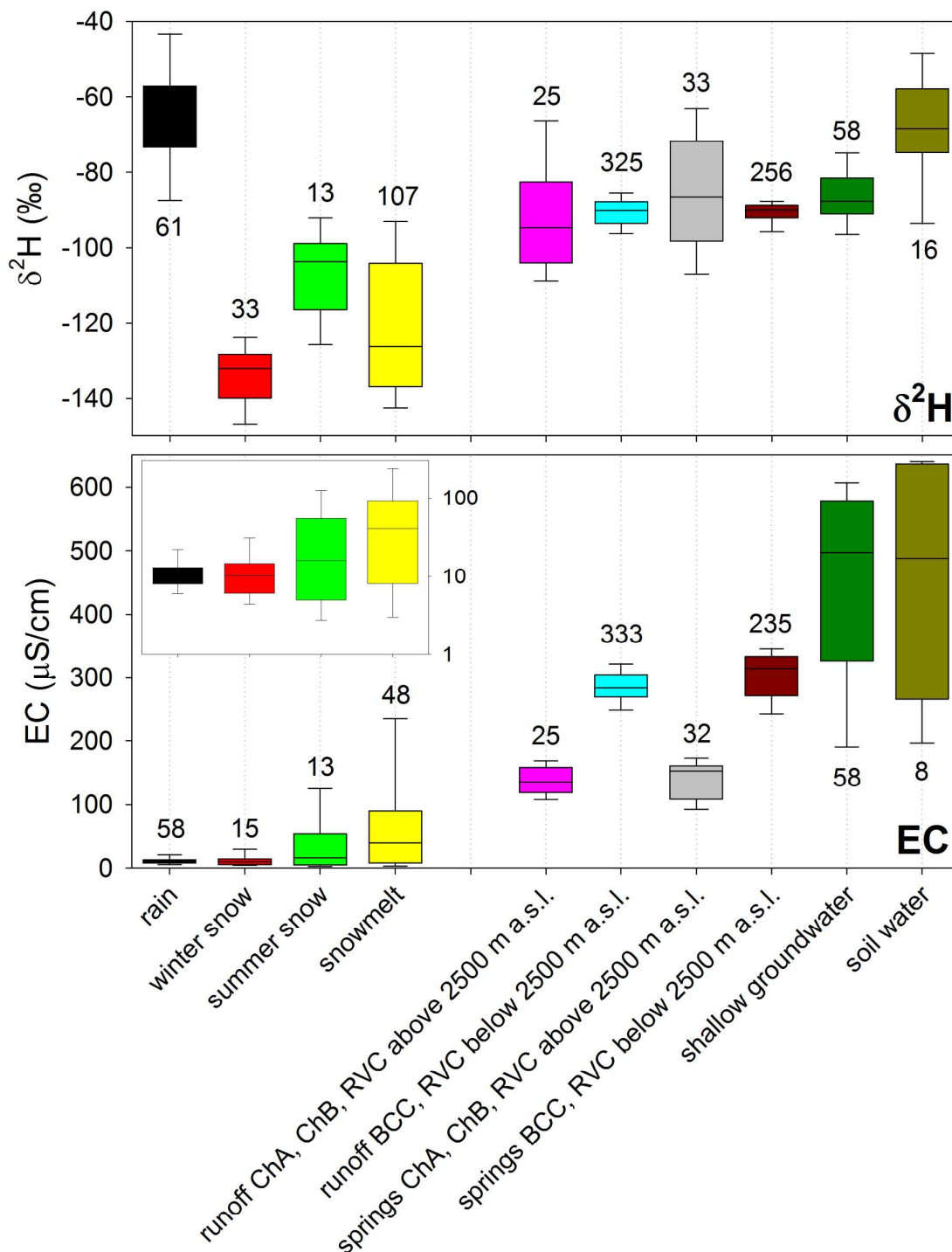


Fig. 4. Box-plot of $\delta^2\text{H}$ (top panel) and EC (bottom panel) of all samples collected in this study. The numbers above or below each box indicate the sample size. In the inset of the bottom panel the box-plot of rain, winter snow, summer snow and snowmelt is reported in log-scale for clarity. The boxes indicate the 25th and 75th percentile, the whiskers indicate the 10th and 90th percentile, the horizontal line within the box marks the median.

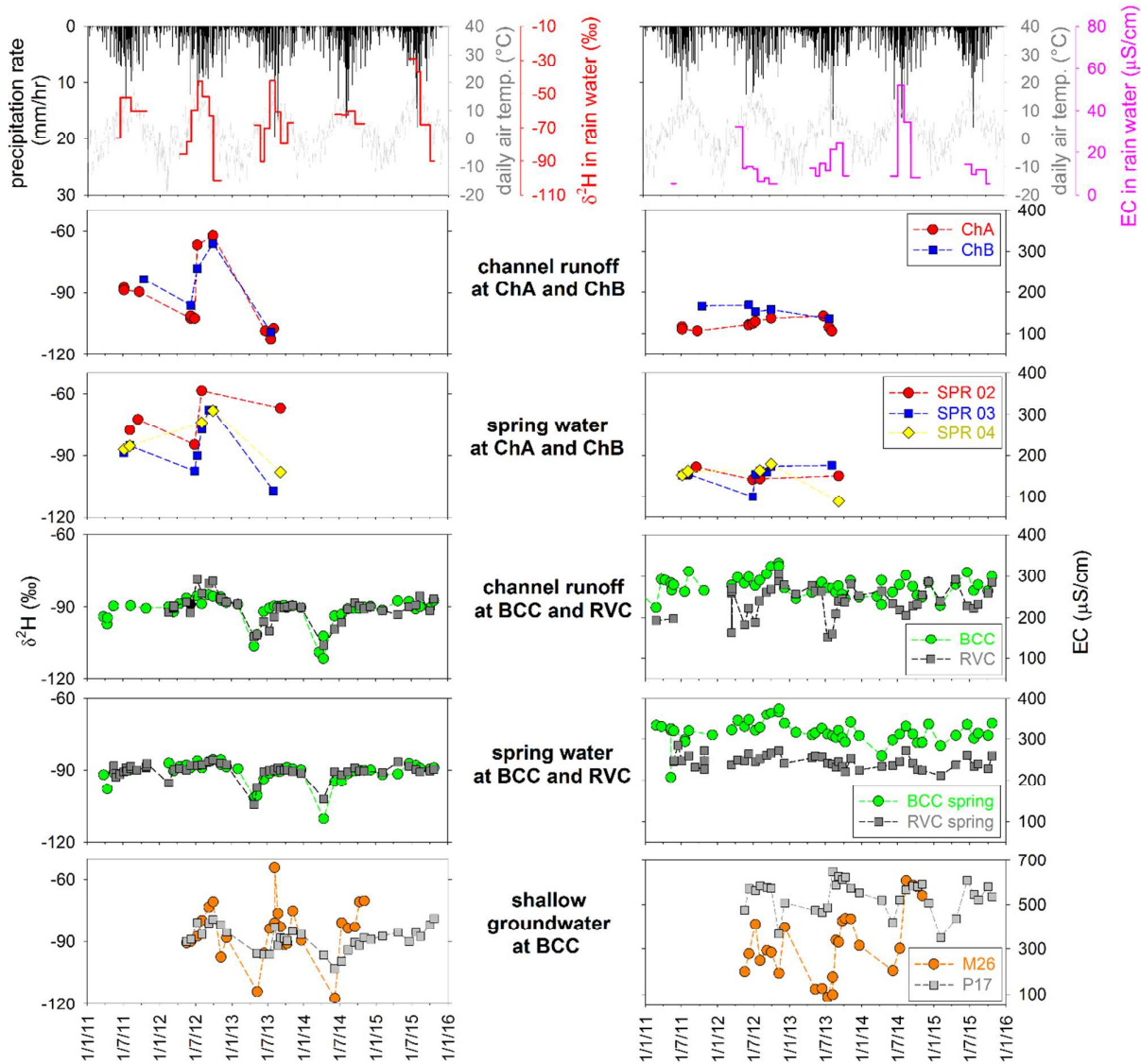


Fig. 5. Hourly time series of precipitation (interpolated values between Arabba and Pordoi pass stations), daily average air temperature (at Pordoi pass station), $\delta^2\text{H}$ in rain water (top panel left) and EC in rain water (top panel right), and $\delta^2\text{H}$ (panels on the left) and EC (panels on the right) of channel runoff, spring water and shallow groundwater samples collected at BCC and in the lower part of RVC in the years 2011-2015. The location for channel runoff at BCC shown here is the outlet, and at RVC shown is the closest to the BCC outlet, which is the only RVC location which we have sampled regularly over the years.

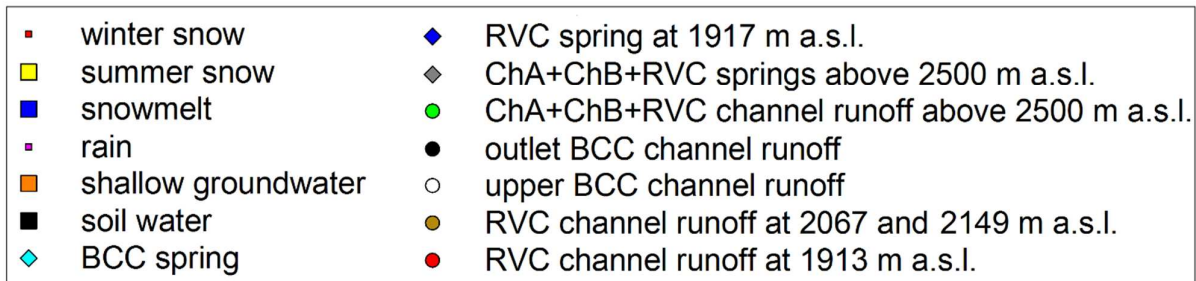
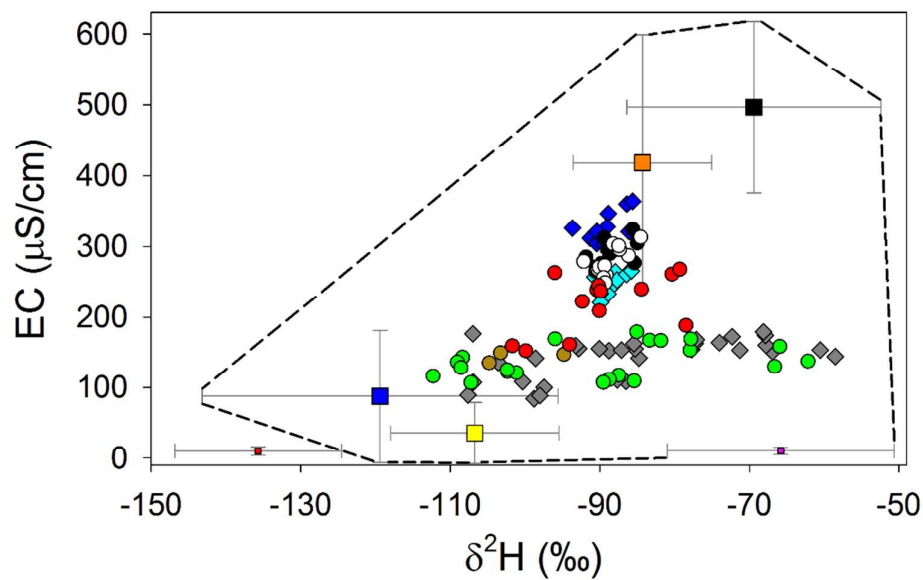


Fig. 6. Mixing-plot of $\delta^2\text{H}$ vs. EC for all water sources sampled in the period June-October 2011-2013 during no-rainy conditions. Soil water, shallow groundwater, snowmelt, summer snow, winter snow and rain water are represented as averages, and error bars indicate the standard deviation. The isotopic composition and EC of rainfall are weighted for the rainfall amount. Winter snow is excluded from the mixing space because it is not a direct hydrological input.

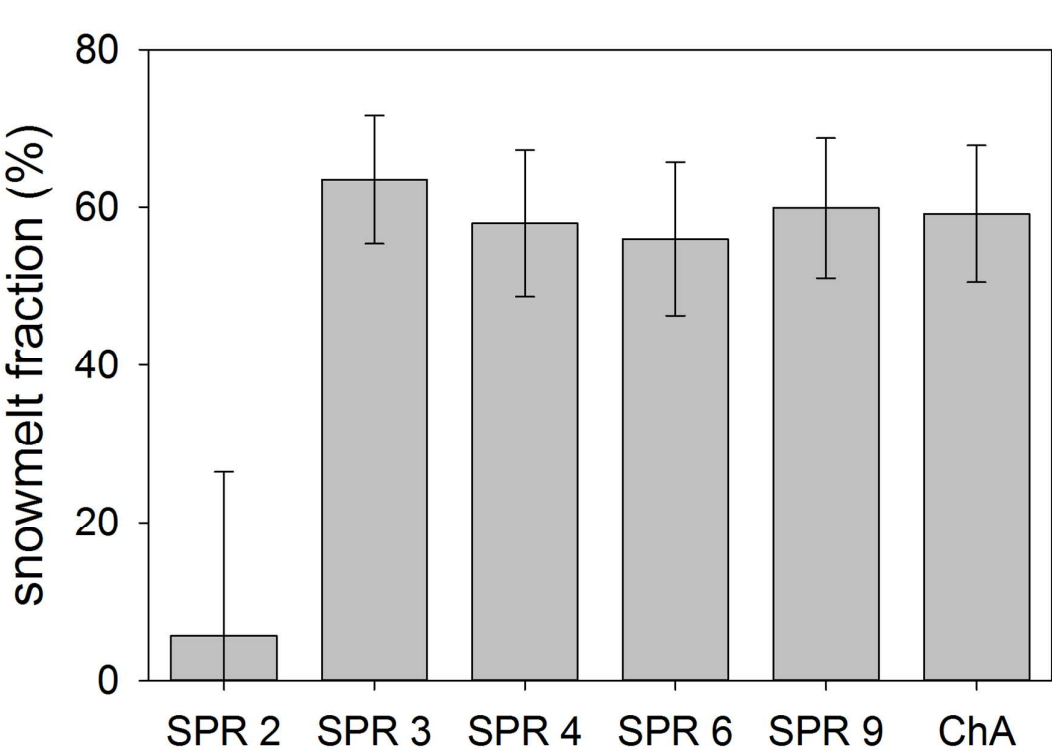


Fig. 7. Snowmelt fraction in spring water and channel runoff sampled in the two rocky subcatchments on 5 July 2011. The error bars indicate the uncertainty.

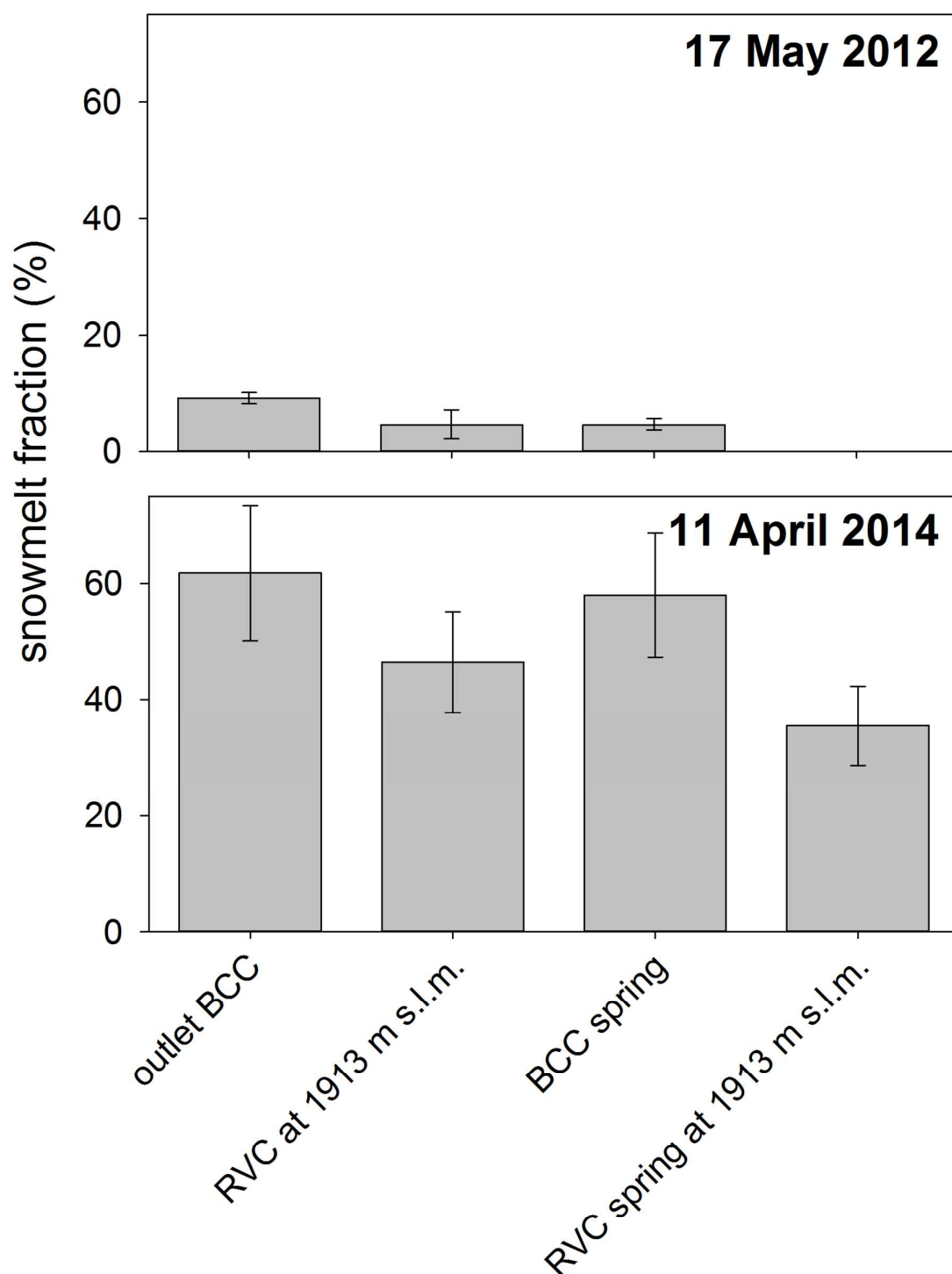
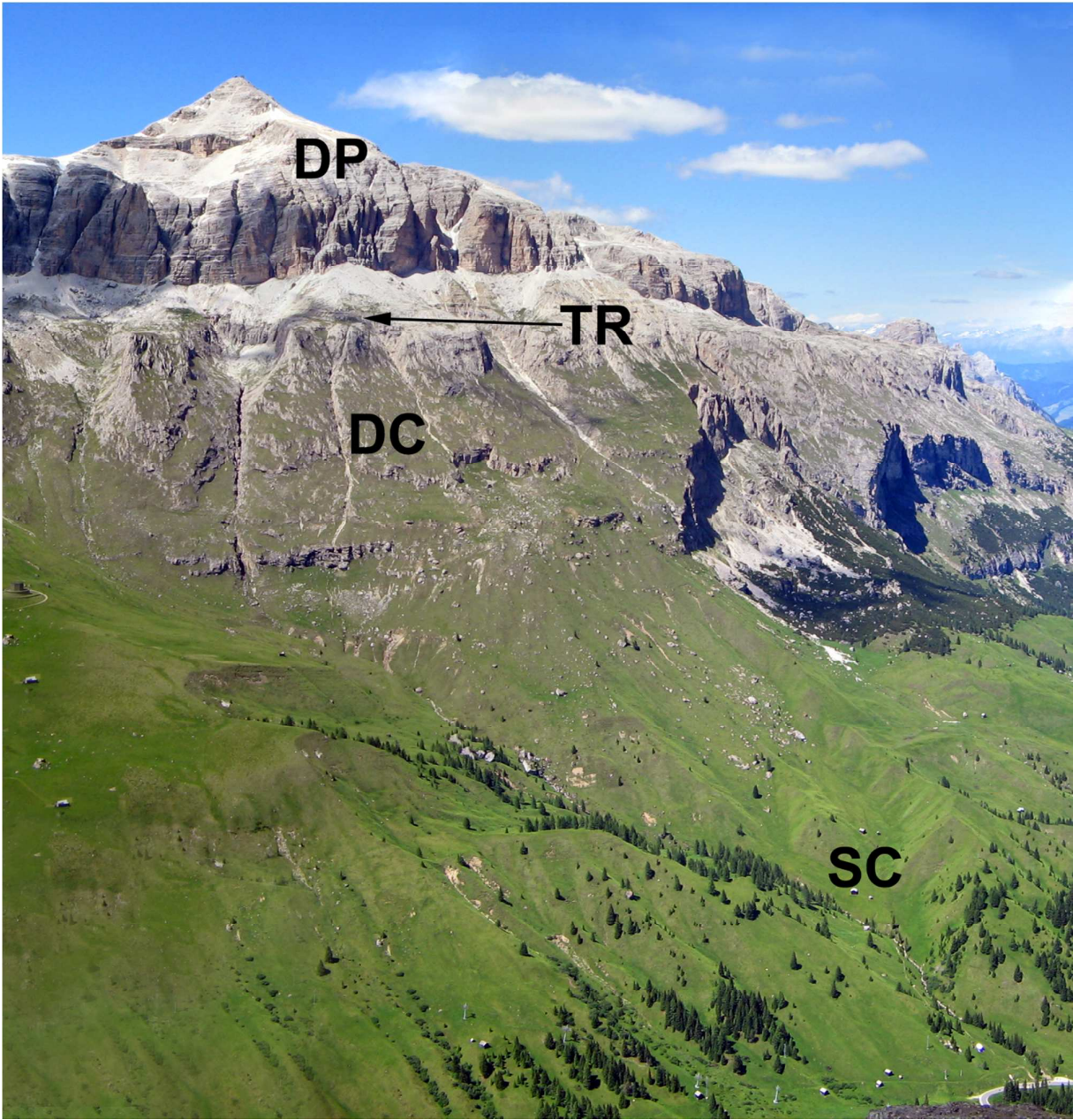


Fig. 8. Snowmelt fraction in channel runoff and spring water sampled at BCC and the bottom part of RVC on 17 May 2012 and 11 April 2014. The error bars indicate the uncertainty.

1
2
3
4
5
6
7
8
9
10
11
12
13
14
15
16
17
18
19
20
21
22
23
24
25
26
27
28
29
30
31
32
33
34
35
36
37
38
39
40
41
42
43
44
45
46
47
48
49
50
51
52
53
54
55
56
57
58
59
60

846 **Supplementary figures**



847
848 Fig. S1. Picture of the Rio Vauz Catchment, with indication of the main geological formations. DP:
849 “Dolomia Principale” (dolomite); TR: “Travenanzes” (formerly “Raibl”: fine graded sandstones,
850 siltstones and claystones); DC: “Dolomia Cassiana” (dolomite); SC: “San Cassiano” (carbonate and
851 terrigenous sandstones and claystones). A more detailed presentation and additional explanations
852 about the main geological formations in the study area are reported in Marchi et al. (2008).

853

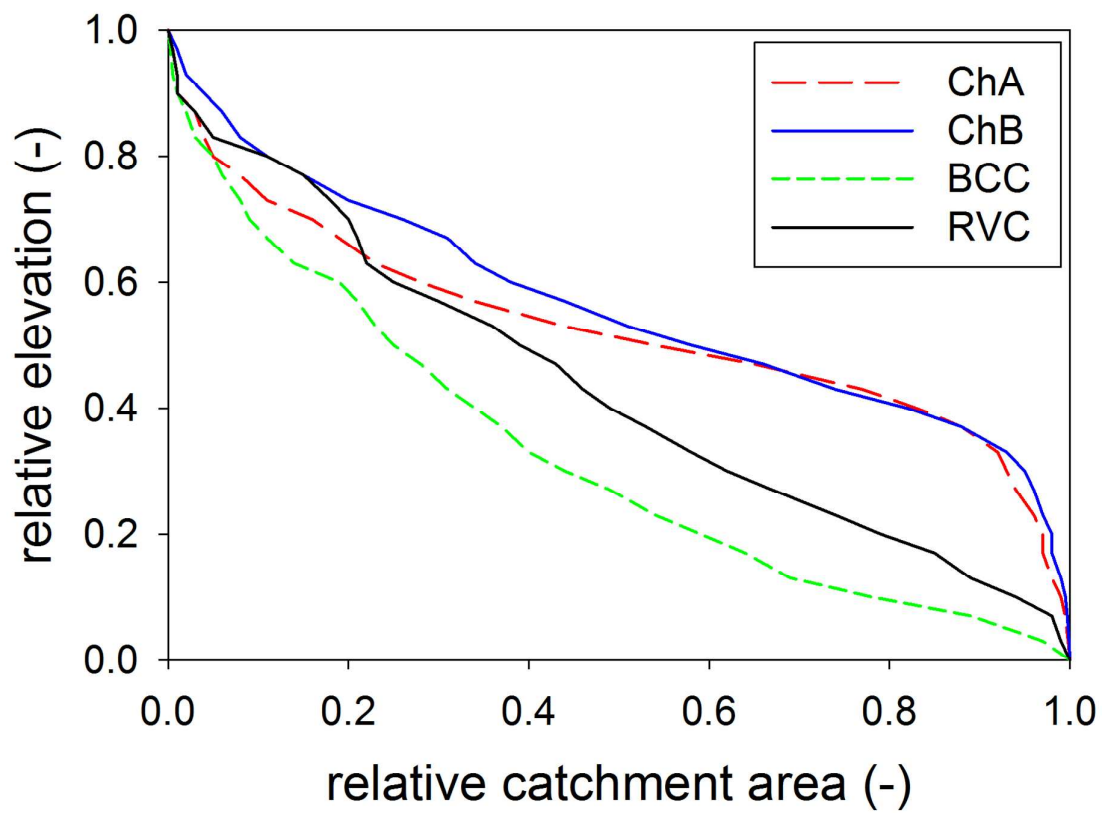


Fig. S2. Dimensionless hypsometric curves of the four study catchments.

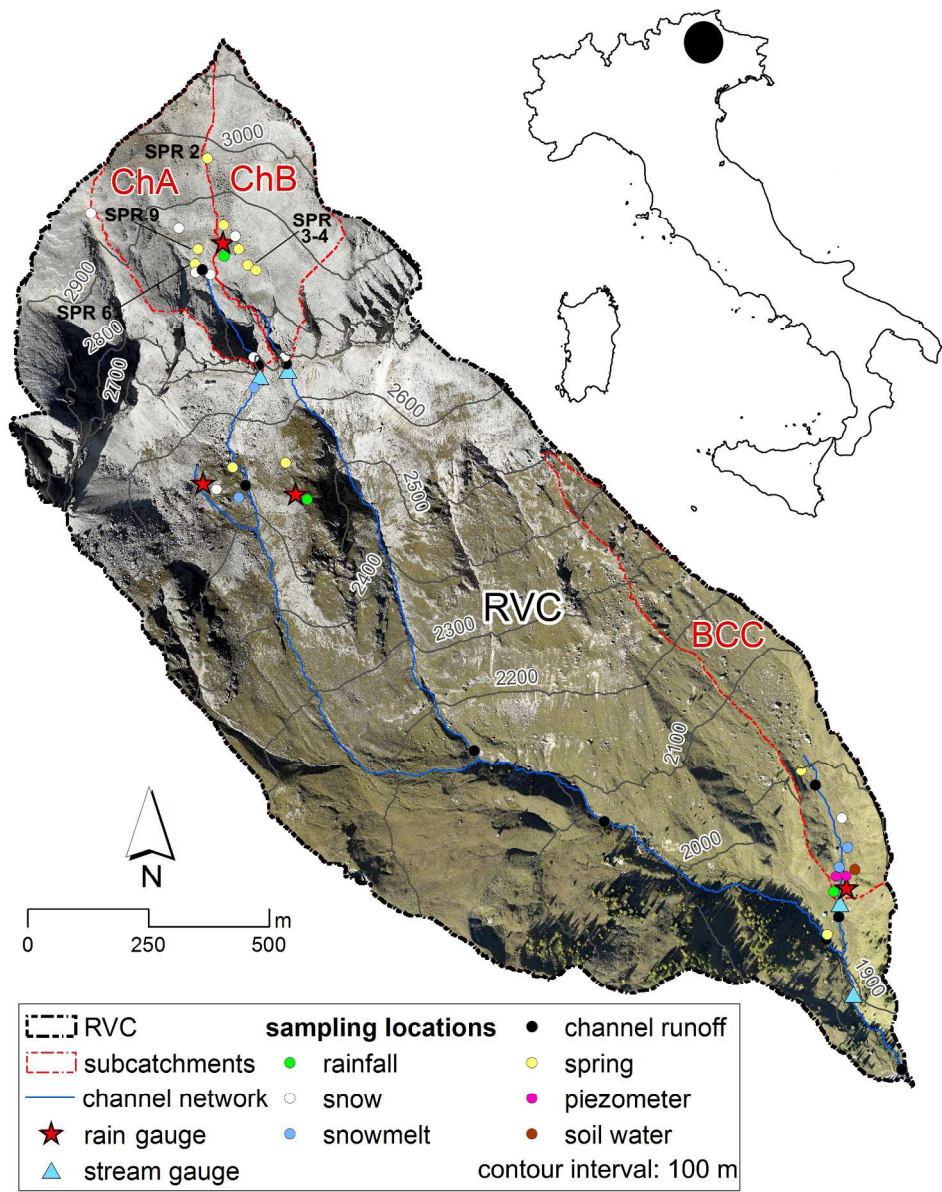


Fig. 1. Rio Vauz Catchment and its selected subcatchments with position of field instruments and sampling locations, and localization in Italy. The springs in the upper part of the catchment for which the two-component mixing model was applied (see Fig. 7) are labelled.

208x264mm (300 x 300 DPI)

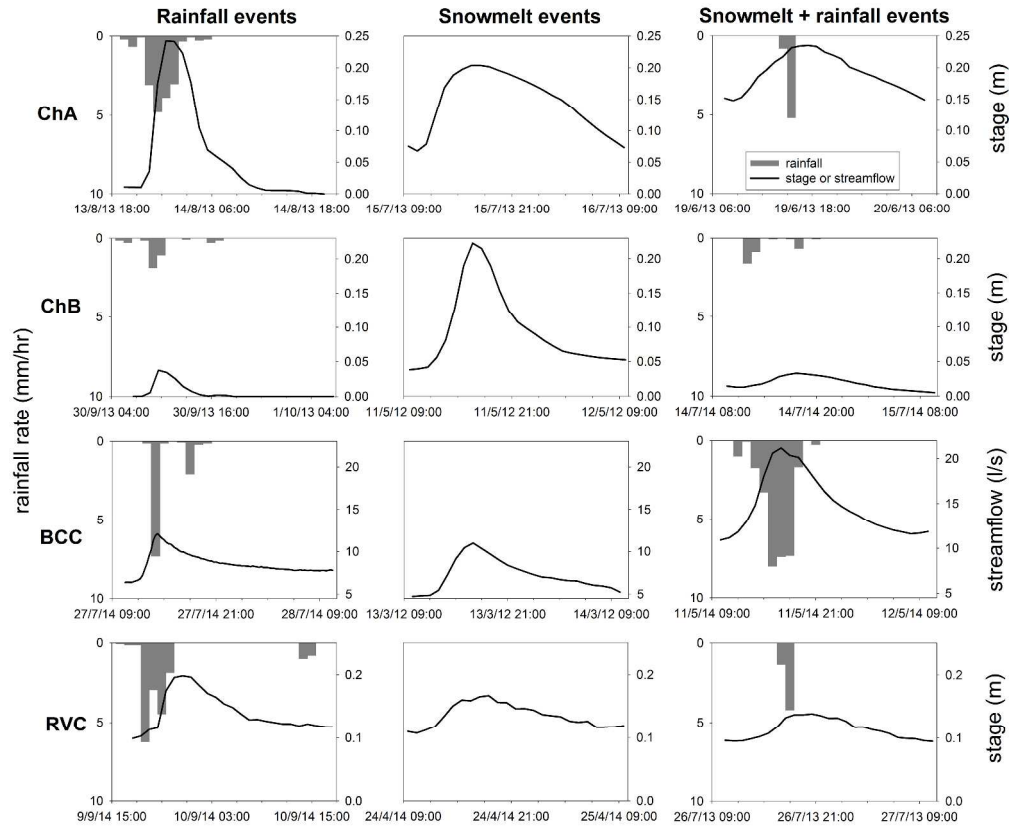


Fig. 2. Examples of rainfall-runoff events, snowmelt-runoff events and mixed-runoff events for all study catchments.

564x466mm (300 x 300 DPI)

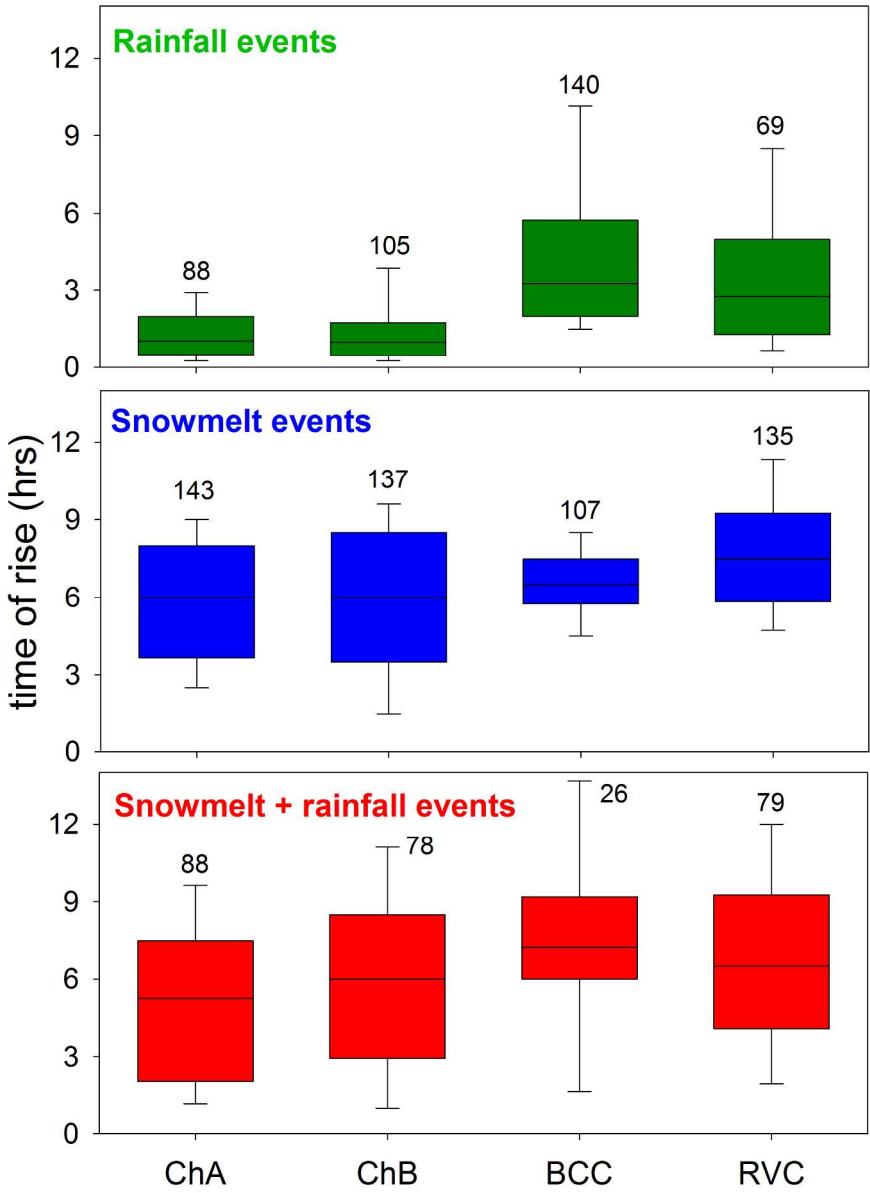


Fig. 3. Box-plot of time of rise for rainfall, snowmelt, and mixed snowmelt-rainfall events for the four study catchments. The numbers above or close to each box indicate the sample size. The boxes indicate the 25th and 75th percentile, the whiskers indicate the 10th and 90th percentile, the horizontal line within the box marks the median.

197x265mm (300 x 300 DPI)

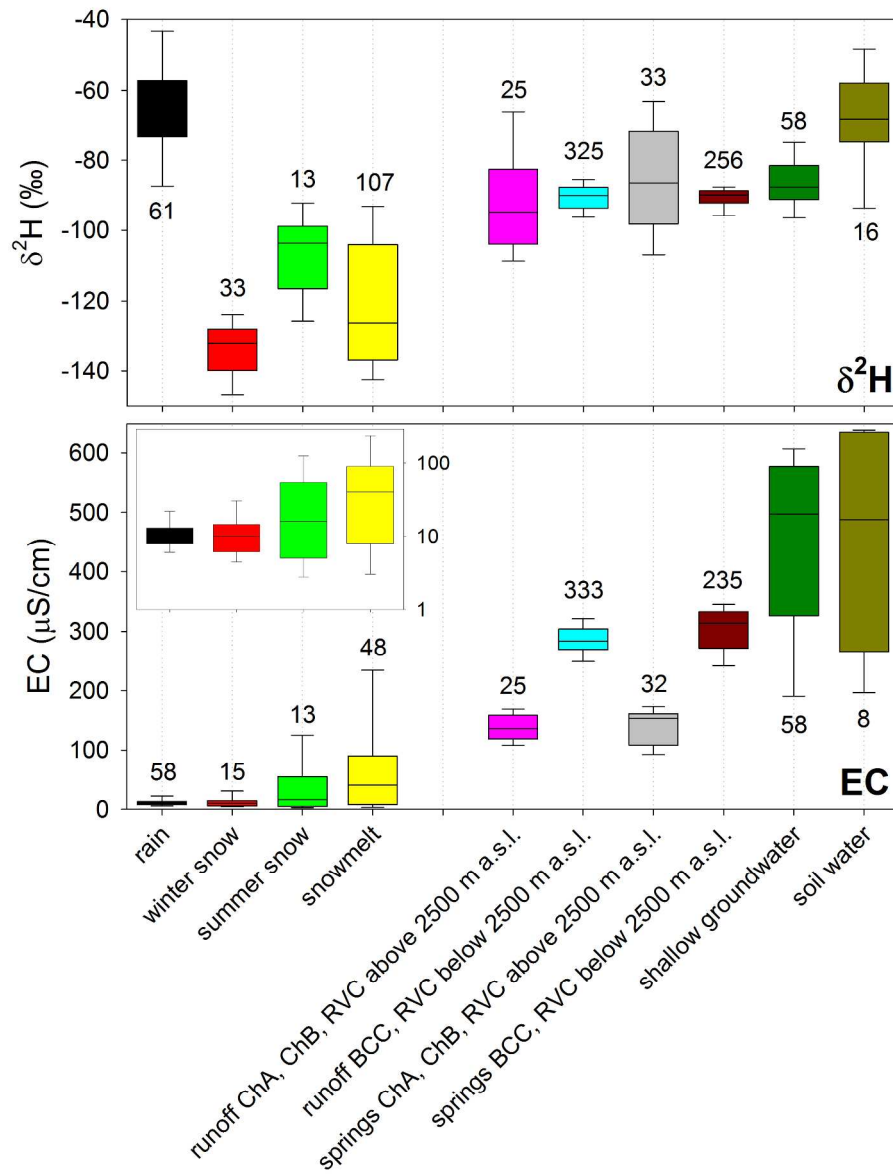


Fig. 4. Box-plot of $\delta^2\text{H}$ (top panel) and EC (bottom panel) of all samples collected in this study. The numbers above or below each box indicate the sample size. In the inset of the bottom panel the box-plot of rain, winter snow, summer snow and snowmelt is reported in log-scale for clarity. The boxes indicate the 25th and 75th percentile, the whiskers indicate the 10th and 90th percentile, the horizontal line within the box marks the median.

212x279mm (300 x 300 DPI)

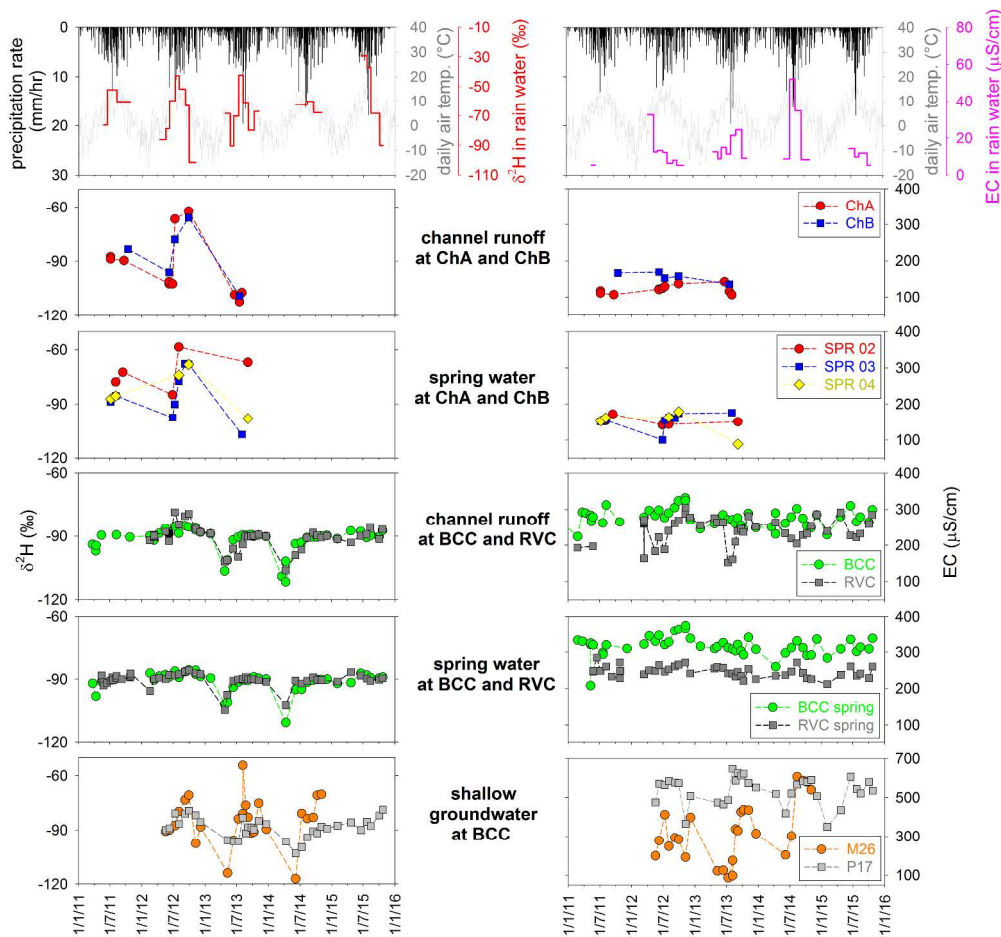


Fig. 5. Hourly time series of precipitation (interpolated values between Arabba and Pordoi pass stations), daily average air temperature (at Pordoi pass station), $\delta^2\text{H}$ in rain water (top panel left) and EC in rain water (top panel right), and $\delta^2\text{H}$ (panels on the left) and EC (panels on the right) of channel runoff, spring water and shallow groundwater samples collected at BCC and in the lower part of RVC in the years 2011-2015. The location for channel runoff at BCC shown here is the outlet, and at RVC shown is the closest to the BCC outlet, which is the only RVC location which we have sampled regularly over the years.

474x448mm (300 x 300 DPI)

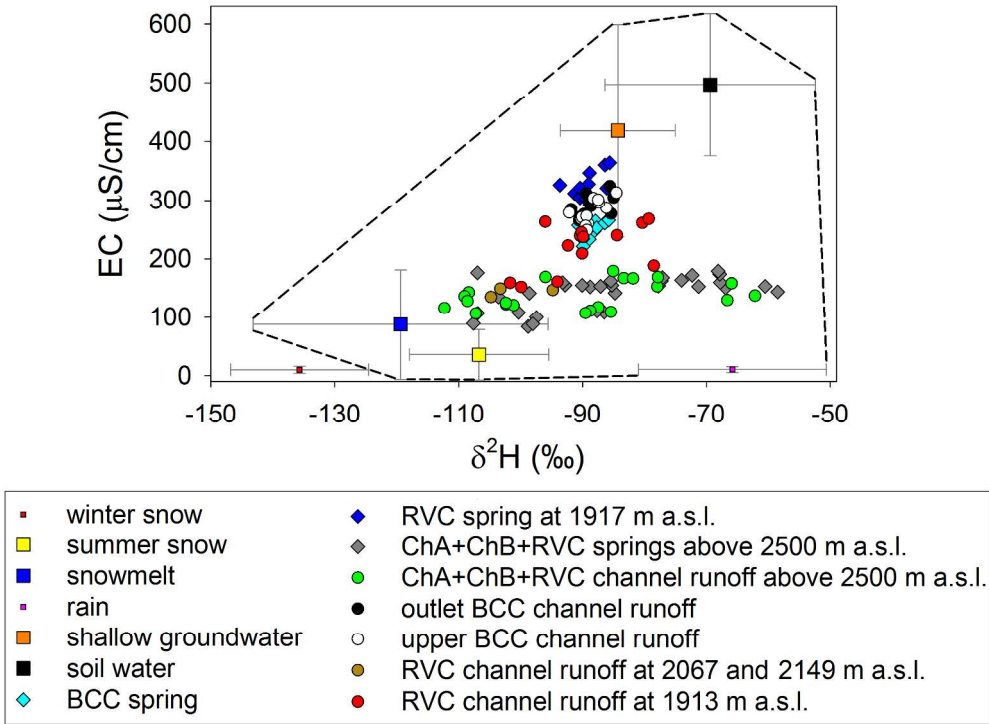


Fig. 6. Mixing-plot of $\delta^2\text{H}$ vs. EC for all water sources sampled in the period June-October 2011-2013 during no-rainy conditions. Soil water, shallow groundwater, snowmelt, summer snow, winter snow and rain water are represented as averages, and error bars indicate the standard deviation. The isotopic composition and EC of rainfall are weighted for the rainfall amount. Winter snow is excluded from the mixing space because it is not a direct hydrological input.

240x180mm (300 x 300 DPI)

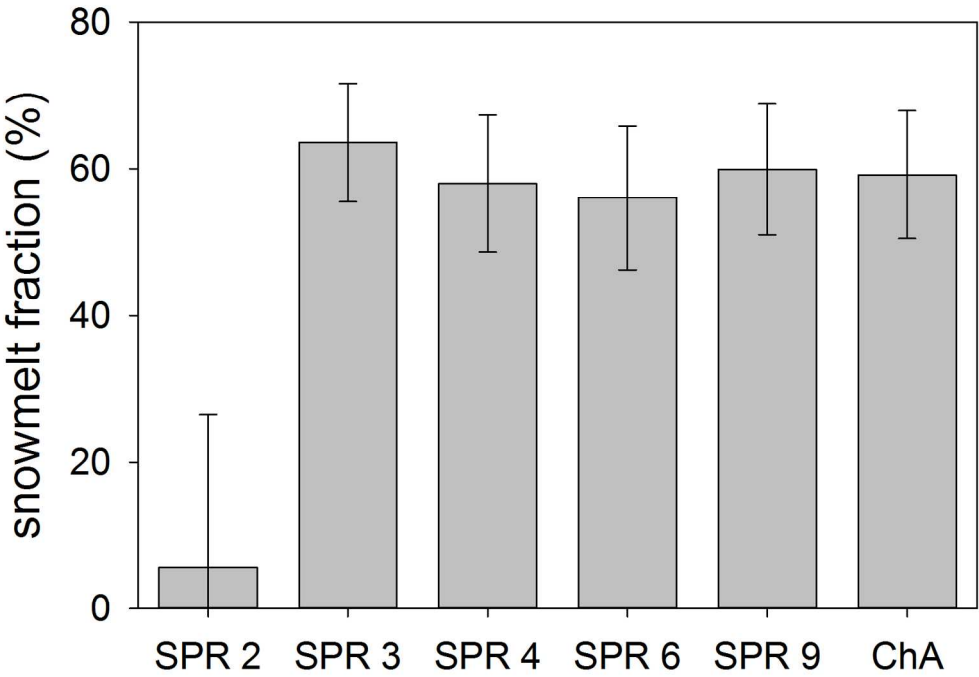


Fig. 7. Snowmelt fraction in spring water and channel runoff sampled in the two rocky subcatchments on 5 July 2011. The error bars indicate the uncertainty.

151x106mm (300 x 300 DPI)

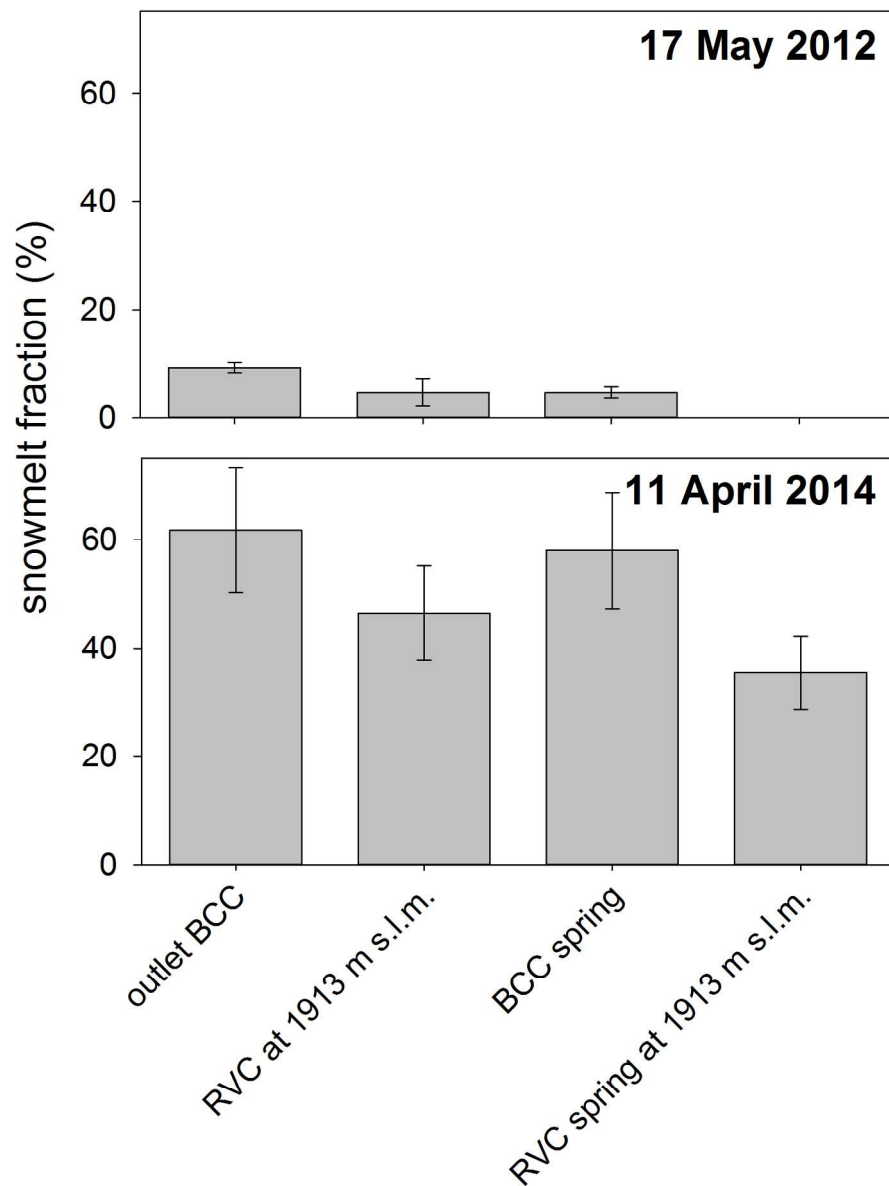


Fig. 8. Snowmelt fraction in channel runoff and spring water sampled at BCC and the bottom part of RVC on 17 May 2012 and 11 April 2014. The error bars indicate the uncertainty.

156x206mm (300 x 300 DPI)

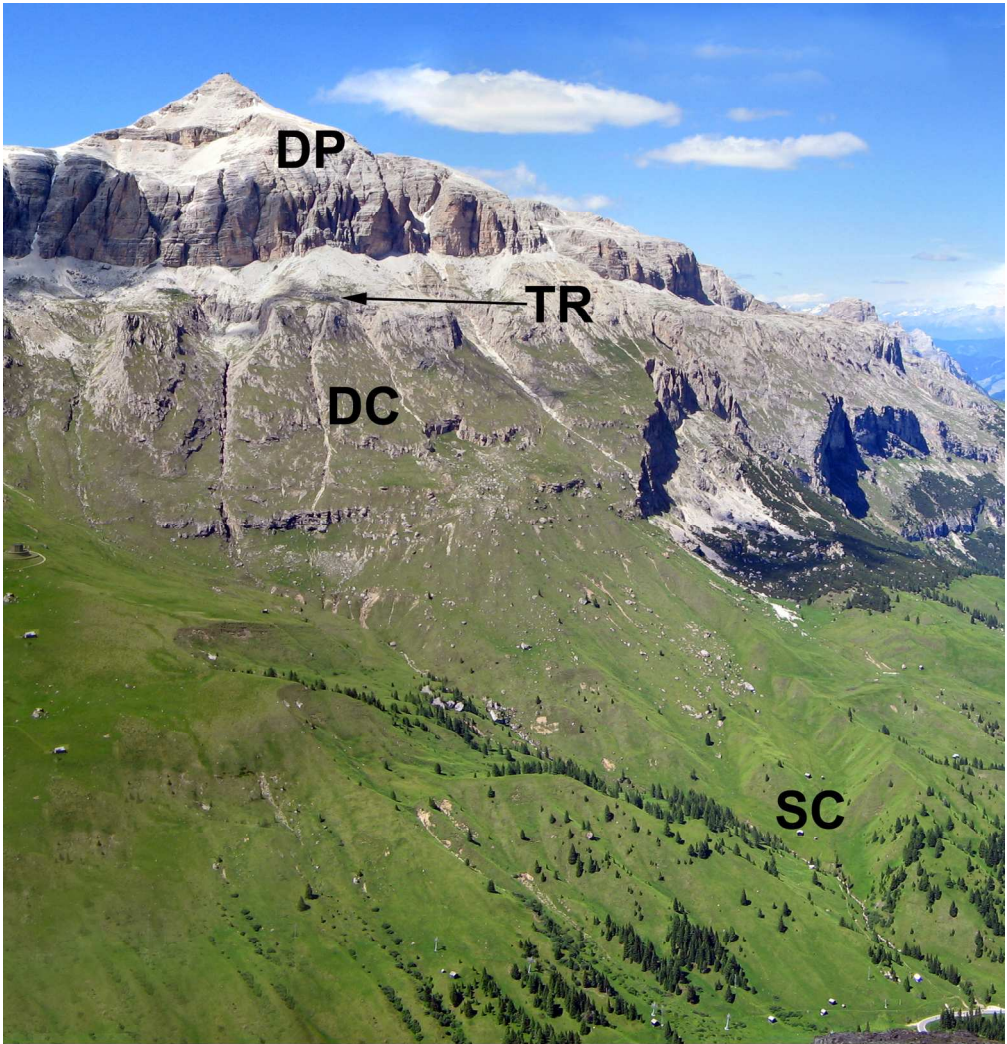


Fig. S1. Picture of the Rio Vauz Catchment, with indication of the main geological formations. DP: "Dolomia Principale" (dolomite); TR: "Travenanzes" (formerly "Raibl": fine graded sandstones, siltstones and claystones); DC: "Dolomia Cassiana" (dolomite); SC: "San Cassiano" (carbonate and terrigenous sandstones and claystones). A more detailed presentation and additional explanations about the main geological formations in the study area are reported in Marchi et al. (2008).

271x282mm (180 x 180 DPI)

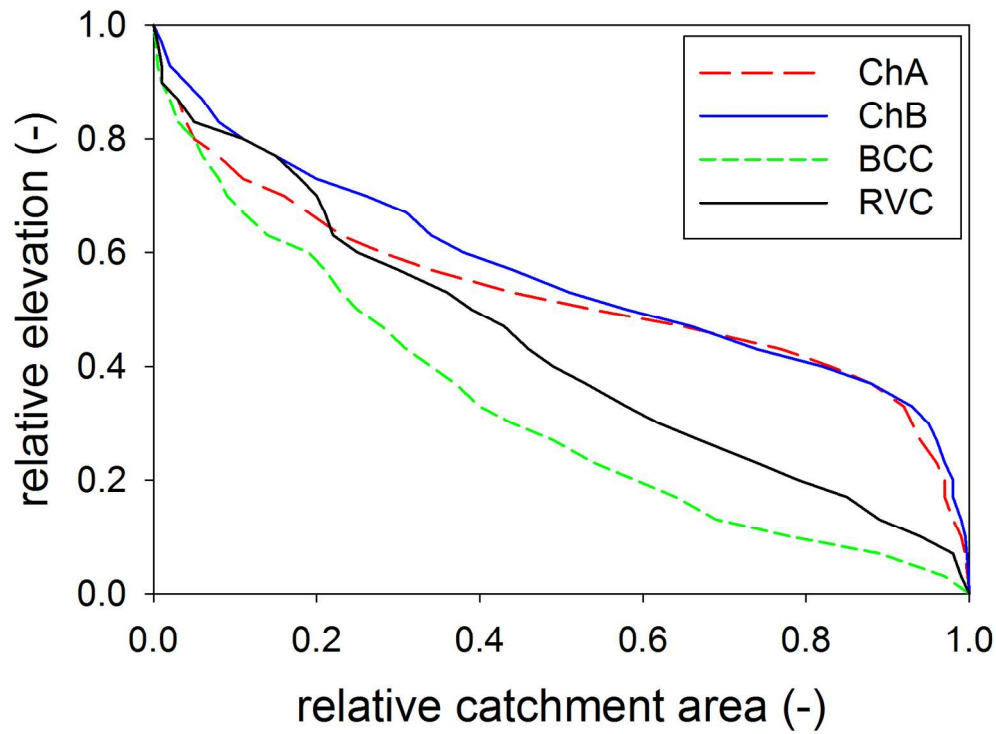


Fig. S2. Dimensionless hypsometric curves of the four study catchments.

155x114mm (300 x 300 DPI)